Nonlinear Dynamic Response and Frequency Analysis of the FG-PCNS With Surface Energy Effects

Sayyid H. HASHEMI KACHAPI
Department of Mechanical Engineering, Babol Noshirvani University of Technology, P.O. Box 484, Shariati Street, Babol, Mazandaran47148-71167, Iran, sha.hashemi.kachapi@gmail.com

Morteza DARDEL
Department of Mechanical Engineering, Babol Noshirvani University of Technology, P.O. Box 484, Shariati Street, Babol, Mazandaran47148-71167, Iran, dardel@nit.ac.ir

Hamidreza MOHAMADI DANIALI
Department of Mechanical Engineering, Babol Noshirvani University of Technology, P.O. Box 484, Shariati Street, Babol, Mazandaran47148-71167, Iran, mohammadi@nit.ac.ir

Alireza FATHI
Department of Mechanical Engineering, Babol Noshirvani University of Technology, P.O. Box 484, Shariati Street, Babol, Mazandaran47148-71167, Iran, fathi@nit.ac.ir

Abstract: - The size-dependent effects on the oscillatory behavior, nonlinear dynamic and frequency response analysis of functionally graded- piezoelectric cylindrical nano-shell (FG-PCNS) as nanoresonator are investigated in the current paper. To this end, Gurtin–Murdoch surface elasticity and von karman-Donnell's theory are used. The governing equations and boundary conditions are derived using Hamilton's principle. The assumed mode method is used for changing the partial differential equations into ordinary differential equations. Also, Complex averaging method combined with arc-length continuation is used to achieve an approximate solution for nonlinear frequency response of the system. The validation of the mention system is achieved with excellent agreements by comparisons with numerical results published in the literature. The parametric study such as the effects of geometrical and material properties, different boundary conditions, the ratio of the length of the nanosystem to the radius L/R, the ratio of nanoshell thickness to radius h_N/R, the ratio of the piezoelectric thickness to the radius h_p/R and amplitude of harmonic force are conducted on natural frequency, nonlinear dynamic and frequency response of the FG piezoelectric nanoresonator.

Keywords: - FG- piezoelectric cylindrical nano-shell, Nonlinear frequency response, Complex averaging method, Arc-length continuation.

1. INTRODUCTION

In recent years, piezoelectric materials play an important role for several applications such as nano-beams, nano-plates, nano-membranes and nano-shells, and are attracting worldwide attention in nanoelectromechanical systems (NEMS) [1-3]. As a result, investigation on the electromechanical characteristics of piezoelectric structures at nanoscale is crucial for NEMS design. The vibration of micro/nano-electromechanical systems is crucial for absorbing the ambient mechanical resources and producing the electric power. To design the nano-sized shell and obtain the desired properties, the vibration character should be addressed. Both molecular dynamics simulation and experimental investigation have invariably shown that the nano-sized effects in the analysis of vibration character of nanostructures cannot be neglected, and since the classical continuum theory is scale-free, it fails to predict the size-dependent response of nano-structures. Consequently, to consider the small scale effect, some non-classical continuum theories have been introduced to develop the size-dependent continuum models [4-9]. The Gurtin–Murdoch surface elasticity theory is non-classical continuum theory applicable to the problems of small-scale structures [8, 9]. This theory can be utilized to study the surface energy effects on the mechanical behavior of nanostructures. In the past two decades, investigating the surface effects on the mechanical behavior of nanostructures has become one of the attractive research areas in nanomechanics, as

evidenced by the large number of publications on this issue [10–29].

According to the surface elasticity theory, Pourkiaee et al. investigated the nonlinear vibration and stability analysis of a doubly clamped piezoelectric nanobeam by using the multiple scales method [10]. The influence of van der Waals forces, piezoelectric voltages and surface effects are investigated on the static equilibria, pull-in voltages and dynamic primary resonances of the nano resonator. In another work, Pourkiaee et al. studied the parametric oscillations of an electrostatically actuated clamped–clamped piezoelectric nanoresonator considering surface effects [11]. Rouhi et al. worked on nonlinear free vibration analysis of circular cylindrical nanoshell with considering Gurtin–Murdoch surface stress theory and shear deformation effects [12]. Investigate the size-dependent free vibration of nano-sized piezoelectric double-shell are presented by Fang et al. by using of the combinations of the electro-elastic surface/interface theory [13]. Also, based on electro-elasticity surface/interface theory, Zhu et al. investigated torsional buckling behavior of FG cylindrical nano-shell covered with piezoelectric nano-layers [14]. Vibration analysis of fluid-conveying nanotubes was presented by Wang [15]. The results show that the surface effects with positive elastic constant or positive residual surface tension tend to increase the natural frequency and critical flow velocity. The effects of small scale and surface effects on nonlinear vibration of boron nitride nano sheet were showed by Ghorbanpour Arani et al. [16]. Surface effects on the dispersion characteristics of elastic waves propagating in an infinite piezoelectric nanoplate are investigated by Zhang et al. [17]. Based on nonlocal piezoelasticity theory, Ghorbanpour Arani et al. [18] worked on dynamic stability of double-walled boron nitride nanotubes (DWBNNTs) conveying viscose fluid by incorporating Euler–Bernoulli beam, Timoshenko beam and cylindrical shell theories. In another article by Nonlinear vibration of smart nano-sandwich viscoelastic structure conveying visco-fluid considering surface effects was studied by Fereidoon et al. [19]. Besides, within the framework of surface elasticity theory, the nonlinear free vibration and nonlinear postbuckling behaviors of nano-plates were studied by Wang and Wang [20]. The nonlinear buckling and postbuckling behaviors of shear deformable nano-shell under radial compressive load were studied by Sahmani et al. based on the surface elasticity theory, and the effect of surface free energy on the critical buckling load and end-shortening was discussed [21].

Due to the importance of vibration characteristics such as natural frequencies and mode shapes in proper design of a structure, the present study focuses on the free vibration analysis of a piezoelectric nano-shell with surface energy effect. Studies on free vibrations of shells are quite extensive. In an excellent monograph by Leissa, researches on the vibration analysis of thin shells before 1970s were reviewed [22]. There are also more recent survey such as Liew et al. [23] and Qatu et al. [24] which review articles about shallow shells and dynamic behavior of composite shells, respectively. Ye et al. presented a unified solution method for the free vibration analysis of composite shallow shells with general elastic boundary conditions [25]. Fazollari [26] developed an analytical formulation for free vibration analysis of doubly curved laminated composite shallow shells by combining the dynamic stiffness method and a higher order shear deformation theory. Mirza and Alizadeh investigated the effects of detached base length on the natural frequencies and modal shapes of cylindrical shells [27]. Loy et al. presented the free vibration analysis of cylindrical shells using an improved version of the differential quadrature method [28]. An analytical procedure to study the free vibration characteristics of thin circular cylindrical shells was presented by Naeem and Sharma, in which Ritz polynomial functions are assumed to model the axial modal dependence and the Rayleigh-Ritz variational approach is employed to formulate the general eigenvalue problem [29].

In the present study, the free and force vibration analysis of a functionally graded- piezoelectric cylindrical nano-shell (FG-PCNS) with arbitrary boundary conditions is investigated. The Gurtin–Murdoch surface elasticity theory is employed to derive the total energy of the nano-shell, and is used to obtain the governing differential equations and also, the assumed mode method is used for discretization and obtaining the governing differential equations. Also, Complex averaging method combined with arc-length continuation is used to achieve an approximate solution for nonlinear frequency response of the system. A variety of new vibration results including the effects of geometrical parameters and material properties on natural frequency, nonlinear dynamic and frequency response for FG-PCNS with non-classical restraints are presented.

2. MATHEMATICAL FORMULATION

A cylindrical nano shell embedded with a piezoelectric layer and subjected to harmonic excitation ($f cos\omega t$) shown in Figure 1 where f and ω are the amplitude and angular frequency of the external excitation. The length of nano shell is L, the geometrical parameters of the cylindrical shell are

mid-surface radius R, thickness of cylindrical shell $2h_N$ and thickness of piezoelectric material layer h_p. With the origin of coordinate system located on the middle surface of nano-shell, the coordinates of a typical point in the axial, circumferential and radius directions are described by x, θ, and z, respectively.

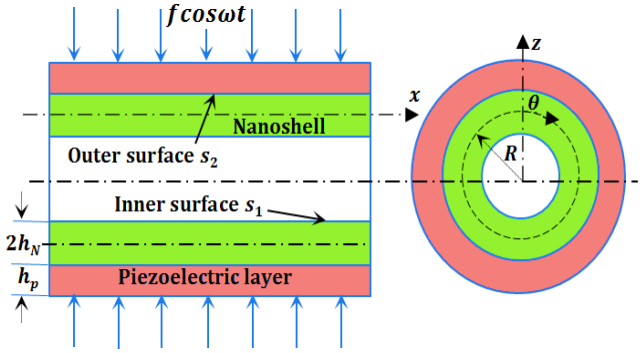

Figure 1. A functionally graded- piezoelectric cylindrical nano-shell (FG-PCNS)

E_N, υ_N and ρ_N represent Young modulus, Poisson ratio and the mass density of cylindrical nano-shell. In the present nano-shell, it is assumed that the material properties E_N, υ_N and ρ_N vary through the thickness of nano-shell according to the power-law function. They are written as

$$E_N = (E_T - E_B)\left(\frac{2z+h_N}{2h_N}\right)^q + E_B \quad (1)$$

$$\upsilon_N = (\upsilon_T - \upsilon_B)\left(\frac{2z+h_N}{2h_N}\right)^q + \upsilon_B \quad (2)$$

$$\rho_N = (\rho_T - \rho_B)\left(\frac{2z+h_N}{2h_N}\right)^q + \rho_B \quad (3)$$

where q is the power-law exponent. The subscripts T and B represent the properties of the nano-shell at the upper and lower layers, respectively.

Young modulus, Poisson ratio, piezoelectric and dielectric constants and the mass density of piezoelectric layer are $E_p, \upsilon_p, e_{31p}, e_{32p}, \eta_{33p}$ and ρ_p. Due to the nano-sized property, the ratio of surface to the volume becomes large, and the surface energy around the shell expresses significant effect on the vibration of nano-structure. According to the electro-elastic surface/interface theory, the surface/interface region adhered to the neighboring solids is several atomic sizes, and has its own electromechanical properties. The surface at the outer piezoelectric layer is denoted by s_2, and the inner surface is denoted by s_1, as shown in Figure 1. The material properties of surface s_2 are Lamé's constants λ^{s_2}, μ^{s_2}, residual stress $\tau_0^{s_2}$ and piezoelectric constants $e_{31p}^{s_2}, e_{32p}^{s_2}$. Those of the inner surface are Lame's constants λ^{s_1}, μ^{s_1}, and residual stress $\tau_0^{s_1}$.

Due to the character of nano-shell, the state of generalized plane stress of shells is assumed, and the normal stress in the radial direction is zero. In the cylindrical nano-shell, the constitutive relation can be expressed as [30, 31];

$$\begin{Bmatrix}\sigma_{xxN}\\ \sigma_{\theta\theta N}\\ \tau_{x\theta N}\end{Bmatrix} = \begin{bmatrix}C_{11N} & C_{12N} & 0\\ C_{21N} & C_{22N} & 0\\ 0 & 0 & C_{66N}\end{bmatrix}\begin{Bmatrix}\varepsilon_{xx}\\ \varepsilon_{\theta\theta}\\ \gamma_{x\theta}\end{Bmatrix} \quad (4)$$
$$or \quad \{\sigma_N\} = [C_N]\{\varepsilon\}$$

In the outside piezoelectric shell, the constitutive relation can be expressed as [30, 31]

$$\begin{Bmatrix}\sigma_{xxp}\\ \sigma_{\theta\theta p}\\ \tau_{x\theta p}\end{Bmatrix} = \begin{bmatrix}C_{11p} & C_{12p} & 0\\ C_{21p} & C_{22p} & 0\\ 0 & 0 & C_{66p}\end{bmatrix}\begin{Bmatrix}\varepsilon_{xx}\\ \varepsilon_{\theta\theta}\\ \gamma_{x\theta}\end{Bmatrix} - \begin{bmatrix}0 & 0 & e_{31p}\\ 0 & 0 & e_{32p}\\ 0 & 0 & 0\end{bmatrix}\begin{Bmatrix}\bar{E}_{xp}\\ \bar{E}_{\theta p}\\ \bar{E}_{zp}\end{Bmatrix} \quad (5)$$
$$\text{or} \quad \{\sigma_p\} = [C_p]\{\varepsilon\} - [e_p]\{\bar{E}_p\},$$

in which the subscripts N and P represent the cylindrical nano-shell and piezoelectric layers, respectively. $\{\bar{E}_p\}$ is the vector of electric field for piezoelectric layers. $[C_N]$ and $[C_p]$are the matrixes of elastic constants, and they can be denoted as

$$C_{11N} = \frac{E_N}{1-\upsilon_N^2} = C_{22N}, C_{12N} = \frac{\upsilon_N E_N}{1-\upsilon_N^2} = C_{21N}, \quad (6)$$
$$C_{66N} = \frac{E_N}{2(1+\upsilon_N)},$$
$$C_{11p} = \frac{E_p}{1-\upsilon_p^2} = C_{22p}, C_{12p} = \frac{\upsilon_p E_p}{1-\upsilon_p^2} = C_{21p}, \quad (7)$$
$$C_{66p} = \frac{E_p}{2(1+\upsilon_p)},$$

Since the piezoelectric layers are very thin, $\bar{E}_{xp}$and $\bar{E}_{\theta p}$are assumed to be zero ($\bar{E}_{xp} = \bar{E}_{\theta p} = 0$), and only the radial component of electric field $\bar{E}_{zp}$is considered. Consequetly, $\{\bar{E}_p\}$ can be written as

$$\begin{Bmatrix}\bar{E}_{xp}\\ \bar{E}_{\theta p}\\ \bar{E}_{zp}\end{Bmatrix} = \begin{Bmatrix}0\\ 0\\ V_p/h_p\end{Bmatrix}, \quad (8)$$

where V_p is the voltage applied to piezoelectric layers. In addition, the voltages at the piezoelectric surface $S_2(z = h_N + h_p)$ and $S_1(z = h_N)$ are $+V_p$ and $-V_p$, respectively. Based on these assumptions mentioned above, the radial component of electric displacement D_{zp} can be presented as

$$D_{zp} = e_{31p}\varepsilon_{xx} + e_{32p}\varepsilon_{\theta\theta} + \eta_{33p}\bar{E}_{zp}, \quad (9)$$

3. NON- CLASSICAL SHELL THEORY

Within the framework of classical shell theory, the displacement fields of the nano-shell can be written as [31]

$$u_x(x,\theta,z) = u(x,\theta) - z\frac{\partial w(x,\theta)}{\partial x}, \quad (10)$$

$$u_\theta(x,\theta,z) = v(x,\theta) - \frac{z}{R}\frac{\partial w(x,\theta)}{\partial \theta}, \quad (11)$$

$$u_z(x,\theta,z) = w(x,\theta), \quad (12)$$

where u, v and w stand for the middle surface displacements in the x , θ and z directions, respectively. The nonlinear deflection and curvatures are defined by von Karman-Donnell's theory as [30, 31]

$$\begin{Bmatrix}\varepsilon_{xx}\\ \varepsilon_{\theta\theta}\\ \gamma_{x\theta}\end{Bmatrix} = \begin{Bmatrix}\varepsilon^0_{xx}\\ \varepsilon^0_{\theta\theta}\\ \gamma^0_{x\theta}\end{Bmatrix} + z\begin{Bmatrix}\kappa_{xx}\\ \kappa_{\theta\theta}\\ \kappa_{x\theta}\end{Bmatrix} = \quad (13)$$

$$\begin{Bmatrix}\frac{\partial u}{\partial x} + \frac{1}{2}\left(\frac{\partial w}{\partial x}\right)^2\\ \frac{1}{R}\left(\frac{\partial v}{\partial \theta} + w\right) + \frac{1}{2R^2}\left(\frac{\partial w}{\partial \theta}\right)^2\\ \frac{1}{R}\frac{\partial u}{\partial \theta} + \frac{\partial v}{\partial x} + \frac{1}{R}\frac{\partial w}{\partial x}\frac{\partial w}{\partial \theta}\end{Bmatrix} - z\begin{Bmatrix}\frac{\partial^2 w}{\partial x^2}\\ \frac{1}{R^2}\frac{\partial^2 w}{\partial \theta^2}\\ \frac{2}{R}\frac{\partial^2 w}{\partial x \partial \theta}\end{Bmatrix},$$

in which ε^0_{xx} ،$\varepsilon^0_{\theta\theta}$ and $\gamma^0_{x\theta}$ are the middle surface strains, and κ_{xx} ,$\kappa_{\theta\theta}$ and $\kappa_{x\theta}$ are the curvature components of the nano-shell.

Since the dimension of the shell is at nanometer scale, the surface effect needs to be considered. On based of the Gurtin–Murdoch surface elasticity theory, the constitute relations for surfaces can be written as [8, 9]

$$\sigma^{s_2}_{\alpha\beta} = \tau^{s_2}_0\delta_{\alpha\beta} + \left(\tau^{s_2}_0 + \lambda^{s_2}\right)\varepsilon_{qq}\delta_{\alpha\beta} \quad (14a)$$
$$+2\left(\mu^{s_2} - \tau^{s_2}_0\right)\varepsilon_{\alpha\beta} + \tau^{s_2}_0 u^{s_2}_{\alpha,\beta} - e^{s_2}_p E_{zp},$$
$$\sigma^{s_2}_{\alpha z} = \tau^{s_2}_0 u^{s_2}_{z,\alpha}, (\alpha,\beta = x,\theta)$$
$$\sigma^{s_1}_{\alpha\beta} = \tau^{s_1}_0\delta_{\alpha\beta} + \left(\tau^{s_1}_0 + \lambda^{s_1}\right)\varepsilon_{qq}\delta_{\alpha\beta} \quad (14b)$$
$$+2\left(\mu^{s_1} - \tau^{s_1}_0\right)\varepsilon_{\alpha\beta} + \tau^{s_1}_0 u^{s_1}_{\alpha,\beta}, \sigma^{s_1}_{\alpha z} = \tau^{s_1}_0 u^{s_1}_{z,\alpha},$$

in which $\delta_{\alpha\beta}$ is the Kronecker delta function. Furthermore, the components of stress at the surfaces can be expressed as

$$\sigma^{s_2}_{xx} = (\lambda^{s_2} + 2\mu^{s_2})\varepsilon_{xx} + \left(\tau^{s_2}_0 + \lambda^{s_2}\right)\varepsilon_{\theta\theta} \quad (15a)$$
$$-\frac{\tau^{s_2}_0}{2}\left(\frac{\partial w}{\partial x}\right)^2 + \tau^{s_2}_0 - e^{s_2}_{31p}E_{zp},$$
$$\sigma^{s_2}_{\theta\theta} = \left(\tau^{s_2}_0 + \lambda^{s_2}\right)\varepsilon_{xx} + (\lambda^{s_2} + 2\mu^{s_2})\varepsilon_{\theta\theta} \quad (15b)$$
$$-\tau^{s_2}_0\left(\frac{w}{R} + \frac{1}{2R^2}\left(\frac{\partial w}{\partial \theta}\right)^2\right) + \tau^{s_2}_0 - e^{s_2}_{32p}E_{zp},$$
$$\sigma^{s_1}_{xx} = (\lambda^{s_1} + 2\mu^{s_1})\varepsilon_{xx} + \left(\tau^{s_1}_0 + \lambda^{s_1}\right)\varepsilon_{\theta\theta} \quad (15c)$$
$$-\frac{\tau^{s_1}_0}{2}\left(\frac{\partial w}{\partial x}\right)^2 + \tau^{s_1}_0,$$
$$\sigma^{s_1}_{\theta\theta} = \left(\tau^{s_1}_0 + \lambda^{s_1}\right)\varepsilon_{xx} + (\lambda^{s_1} + 2\mu^{s_1})\varepsilon_{\theta\theta} \quad (15d)$$
$$-\tau^{s_1}_0\left(\frac{w}{R} + \frac{1}{2R^2}\left(\frac{\partial w}{\partial \theta}\right)^2\right) + \tau^{s_1}_0,$$
$$\sigma^{s_i}_{x\theta} = \mu^{s_i}\gamma_{x\theta} - \tau^{s_i}_0\left(\frac{\partial v}{\partial x} + \frac{1}{2R}\frac{\partial w}{\partial x}\frac{\partial w}{\partial \theta} - \frac{z}{R}\frac{\partial^2 w}{\partial x \partial \theta}\right), \quad (15e)$$
$$\sigma^{s_i}_{xz} = \tau^{s_i}_0\frac{\partial w}{\partial x}, \quad (15f)$$
$$\sigma^{s_i}_{\theta x} = \mu^{s_i}\gamma_{x\theta} - \tau^{s_i}_0\begin{pmatrix}\frac{1}{R}\frac{\partial u}{\partial \theta} + \frac{1}{2R}\frac{\partial w}{\partial x}\frac{\partial w}{\partial \theta}\\ -\frac{z}{R}\frac{\partial^2 w}{\partial x \partial \theta}\end{pmatrix}, \quad (15g)$$
$$\sigma^{s_i}_{\theta z} = \frac{\tau^{s_i}_0}{R}\frac{\partial w}{\partial \theta}, (i = 1,2), \quad (15h)$$

Based on the classical continuum models, σ_{zz} is neglected due to its small value as compared to other normal stress components. But, in the present nonclassical continuum model, this assumption does not satisfy the surface conditions. Thus, it is supposed that σ_{zz} varies linearly through the thickness and satisfies the balance conditions on the surfaces [8, 9], i.e.

$$\sigma_{zz} = \frac{1}{2}\begin{pmatrix}\left(\frac{\partial \sigma^{s_2}_{xz}}{\partial x} + \frac{1}{R}\frac{\partial \sigma^{s_2}_{\theta z}}{\partial \theta} - \rho^{s_2}\frac{\partial^2 w}{\partial t^2}\right)\\ -\left(\frac{\partial \sigma^{s_1}_{xz}}{\partial x} + \frac{1}{R}\frac{\partial \sigma^{s_1}_{\theta z}}{\partial \theta} - \rho^{s_1}\frac{\partial^2 w}{\partial t^2}\right)\end{pmatrix} \quad (16)$$
$$+\frac{1}{2h_N + h_p}\begin{pmatrix}\left(\frac{\partial \sigma^{s_2}_{xz}}{\partial x} + \frac{1}{R}\frac{\partial \sigma^{s_2}_{\theta z}}{\partial \theta} - \rho^{s_2}\frac{\partial^2 w}{\partial t^2}\right)\\ +\left(\frac{\partial \sigma^{s_1}_{xz}}{\partial x} + \frac{1}{R}\frac{\partial \sigma^{s_1}_{\theta z}}{\partial \theta} - \rho^{s_1}\frac{\partial^2 w}{\partial t^2}\right)\end{pmatrix}z,$$

For simplification, the material properties of surfaces and interfaces are selected as

$$\tau^{s_1}_0 = \tau^{s_2}_0 = \tau^s_0, \lambda^{s_1} = \lambda^{s_2} = \lambda^s, \quad (17)$$
$$\mu^{s_1} = \mu^{s_2} = \mu^s, e^{s_2}_{31p} = e^s_{31p}, e^{s_2}_{32p} = e^s_{32p},$$

By means of Eqs. (15) and (16), σ_{zz} can be rewritten as

$$\sigma_{zz} = \left(\frac{(\tau^{s_2}_0 - \tau^{s_1}_0)}{2} + \frac{z(\tau^{s_2}_0 + \tau^{s_1}_0)}{2h_N + h_p}\right) \times \left(\frac{\partial^2 w}{\partial x^2} + \frac{1}{R^2}\frac{\partial^2 w}{\partial \theta^2}\right) \quad (18)$$
$$+\left(\frac{(\rho^{s_1} - \rho^{s_2})}{2} - \frac{z(\rho^{s_1} + \rho^{s_2})}{2h_N + h_p}\right)\frac{\partial^2 w}{\partial t^2},$$

According to Eq. (18), the normal stresses σ_{xx} and $\sigma_{\theta\theta}$ Eqs. (4) and (5) can be rewrite ten as

$$\sigma_{xxN} = C_{11N}\varepsilon_{xx} + C_{12N}\varepsilon_{\theta\theta} + \frac{\upsilon_N\sigma_{zz(N,p)}}{1-\upsilon_N}, \quad (19a)$$

$$\sigma_{\theta\theta N} = C_{21N}\varepsilon_{xx} + C_{22N}\varepsilon_{\theta\theta} + \frac{\upsilon_N\sigma_{zz(N,p)}}{1-\upsilon_N}, \quad (19b)$$

$$\sigma_{x\theta N} = C_{66N}\gamma_{x\theta}, \quad (19c)$$

$$\sigma_{xxp} = C_{11p}\varepsilon_{xx} + C_{12p}\varepsilon_{\theta\theta} - e_{31p}\bar{E}_{xp}, \quad (19d)$$
$$+\frac{\upsilon_p\sigma_{zz(N,p)}}{1-\upsilon_p}$$

$$\sigma_{\theta\theta p} = C_{21p}\varepsilon_{xx} + C_{22p}\varepsilon_{\theta\theta} - e_{32p}\bar{E}_{\theta p}, \quad (19e)$$
$$+\frac{\upsilon_N\sigma_{zz(N,p)}}{1-\upsilon_p}$$

$$\sigma_{x\theta p} = C_{66p}\gamma_{x\theta}, \quad (19f)$$

4. GOVERNING EQUATIONS

In this section, the governing equations of motion of the piezoelectric cylindrical nanoshell are obtained by applying the assumed mode method. The total strain energy considering the surface stress effect is expressed as:

$$\pi = \frac{1}{2}\int_0^L \int_0^{2\pi} \int_{-h_N}^{h_N} \left(\sigma_{ijN}\varepsilon_{ij}\right) R dz d\theta dx, \quad (20)$$
$$\frac{1}{2}\int_0^L \int_0^{2\pi} \int_{h_N}^{h_N+h_p} \left(\sigma_{ijp}\varepsilon_{ij} - \bar{E}_{zp}D_{zp}\right) R dz d\theta dx +$$
$$\frac{1}{2}\int_0^L \int_0^{2\pi} \left(\sigma_{ij}^{s_2}\varepsilon_{ij} - \bar{E}_{zp}D_i^{s_2}\right)\left(R + h_N + h_p\right) d\theta dx$$
$$+\frac{1}{2}\int_0^L \int_0^{2\pi} \left(\sigma_{ij}^{s_1}\varepsilon_{ij}\right)(R - h_N) d\theta dx =$$
$$\frac{1}{2}\int_0^L \int_0^{2\pi} \begin{Bmatrix} N_{xx}\varepsilon_{xx}^0 + N_{\theta\theta}\varepsilon_{\theta\theta}^0 + N_{x\theta}\gamma_{x\theta}^0 \\ +M_{xx}\kappa_{xx} + M_{\theta\theta}\kappa_{\theta\theta} + M_{x\theta}\kappa_{x\theta} \\ +\eta_{33}\bar{E}_{zp}^2 h_p \end{Bmatrix} R d\theta dx,$$

In addition, the kinetic energy of the nanoshell can be formulated as:

$$T = \frac{1}{2}\iint \left\{ I\left(\left(\frac{\partial u}{\partial t}\right)^2 + \left(\frac{\partial v}{\partial t}\right)^2 + \left(\frac{\partial w}{\partial t}\right)^2\right)\right\} R d\theta dx, \quad (21)$$

where

$$I = \int_{-h_N}^{h_N} \rho_N\, dz + \int_{h_N}^{h_N+h_p} \rho_p\, dz + \rho^s = 2\rho_N h_N + \rho_p h_p + \rho^{s_2}|_{z=-h_N} + \rho^{s_1}|_{z=h_N+h_p} \quad (22)$$

which ρ_N, ρ_p and ρ^s are the mass density of nanoshell, piezoelectric layer and surfaces, respectively. Also, the work done by the external harmonic excitation and the potential due to external electric voltage respectively, can be expressed as [32]

$$W_f = \int_0^L \int_0^{2\pi} (f\cos\omega t)\, wR d\theta dx, \quad (23)$$

$$W_p = \frac{1}{2}\int_0^L \int_0^{2\pi} \begin{bmatrix} N_{xp}\left(\frac{\partial w}{\partial x}\right)^2 \\ +\frac{1}{R^2}N_{\theta p}\left(\frac{\partial w}{\partial \theta}\right)^2 \end{bmatrix} R d\theta dx, \quad (24)$$

where N_{xp} and $N_{\theta p}$ are the axial and circumferential electrical forces induced by the uniform external electric voltage V_p, respectively.

In Eq. (20), the stresses and moment resultants are defined as

$$(N_{xx}, N_{\theta\theta}, N_{x\theta}) = \int_{-h_N}^{h_N} \sigma_{ijN}\, dz \quad (25a)$$
$$+\int_{h_N}^{h_N+h_p} \sigma_{ijp}\, dz + \sigma_{s_1} + \sigma_{s_2} = (N_{xN}, N_{\theta N}, N_{x\theta N}) +$$
$$\left(N_{xp}, N_{\theta p}, N_{x\theta p}\right) + (\sigma_{xx}, \sigma_{\theta\theta}, (1/2)(\sigma_{x\theta} + \sigma_{\theta x}))_{s_1}$$
$$+(\sigma_{xx}, \sigma_{\theta\theta}, (1/2)(\sigma_{x\theta} + \sigma_{\theta x}))_{s_2},$$
$$(M_{xx}, M_{\theta\theta}, M_{x\theta}) = \int_{-h_N}^{h_N} \sigma_{ijN}\, z dz \quad (25b)$$
$$+\int_{h_N}^{h_N+h_p} \sigma_{ijp}\, z dz + \sigma_{s_2}\left(h_N + h_p\right) - \sigma_{s_1} h_N =$$
$$= (M_{xN}, M_{\theta N}, M_{x\theta N}) + \left(M_{xp}, M_{\theta p}, M_{x\theta p}\right)$$
$$+(\sigma_{xx}, \sigma_{\theta\theta}, (1/2)(\sigma_{x\theta} + \sigma_{\theta x}))_{s_2}\left(h_N + h_p\right)$$
$$-(\sigma_{xx}, \sigma_{\theta\theta}, (1/2)(\sigma_{x\theta} + \sigma_{\theta x}))_{s_1} h_N,$$
$$N_{xx} = A_{11}\varepsilon_{xx}^0 + A_{12}\varepsilon_{\theta\theta}^0 + B_{11}\kappa_{xx} + B_{12}\kappa_{\theta\theta} \quad (25c)$$
$$-\frac{1}{2}\left(\tau_0^{s_1} + \tau_0^{s_2}\right)\left(\frac{\partial w}{\partial x}\right)^2 + \left(\tau_0^{s_1} + \tau_0^{s_2} - N_{xp}\right) +$$
$$F_{11}^*\left(\frac{\partial^2 w}{\partial x^2} + \frac{1}{R^2}\frac{\partial^2 w}{\partial \theta^2}\right) + J_{11}^*\frac{\partial^2 w}{\partial t^2},$$
$$N_{\theta\theta} = A_{21}\varepsilon_{xx}^0 + A_{22}\varepsilon_{\theta\theta}^0 + B_{21}\kappa_{xx} + B_{22}\kappa_{\theta\theta} \quad (25d)$$
$$-\frac{1}{2}\left(\tau_0^{s_1} + \tau_0^{s_2}\right)\left(\frac{2w}{R} + \frac{1}{R^2}\left(\frac{\partial w}{\partial \theta}\right)^2\right) +$$
$$\left(\tau_0^{s_1} + \tau_0^{s_2} - N_{\theta p}\right) + F_{11}^*\left(\frac{\partial^2 w}{\partial x^2} + \frac{1}{R^2}\frac{\partial^2 w}{\partial \theta^2}\right) + J_{11}^*\frac{\partial^2 w}{\partial t^2},$$
$$N_{x\theta} = A_{66}\gamma_{x\theta}^0 + B_{66}\kappa_{x\theta}, \quad (25e)$$

$$M_{xx} = B_{11}\varepsilon_{xx}^0 + B_{12}\varepsilon_{\theta\theta}^0 + D_{11}\kappa_{xx} \quad (25f)$$
$$+D_{12}\kappa_{\theta\theta} + \tau_0^{s_2}\left(1 - \frac{1}{2}\left(\frac{\partial w}{\partial x}\right)^2\right)\left(h_N + h_p\right) -$$
$$\tau_0^{s_1}\left(1 - \frac{1}{2}\left(\frac{\partial w}{\partial x}\right)^2\right) h_N - M_{xp} +$$
$$E_{11}^*\left(\frac{\partial^2 w}{\partial x^2} + \frac{1}{R^2}\frac{\partial^2 w}{\partial \theta^2}\right) + G_{11}^*\frac{\partial^2 w}{\partial t^2},$$
$$M_{\theta\theta} = B_{21}\varepsilon_{xx}^0 + B_{22}\varepsilon_{\theta\theta}^0 + D_{21}\kappa_{xx} + D_{22}\kappa_{\theta\theta} \quad (25g)$$
$$+\tau_0^{s_2}\left(1 - \frac{1}{2}\left(\frac{2w}{R} + \frac{1}{R^2}\left(\frac{\partial w}{\partial \theta}\right)^2\right)\right)\left(h_N + h_p\right) -$$
$$\tau_0^{s_1}\left(1 - \frac{1}{2}\left(\frac{2w}{R} + \frac{1}{R^2}\left(\frac{\partial w}{\partial \theta}\right)^2\right)\right) h_N - M_{\theta p} +$$
$$E_{11}^*\left(\frac{\partial^2 w}{\partial x^2} + \frac{1}{R^2}\frac{\partial^2 w}{\partial \theta^2}\right) + G_{11}^*\frac{\partial^2 w}{\partial t^2},$$
$$M_{x\theta} = B_{66}\gamma_{x\theta}^0 + D_{66}\kappa_{x\theta}, \quad (25h)$$

in which

$$A_{ij} = A_{ijN} + A_{ijp} + A_{ij}^*, \quad (26a)$$
$$B_{ij} = B_{ijN} + B_{ijp} + B_{ij}^*, \quad (26b)$$
$$D_{ij} = D_{ijN} + D_{ijp} + D_{ij}^*, \quad (26c)$$
$$F_{11}^* = F_{11N}^* + F_{11p}^*, \quad (26d)$$
$$J_{11}^* = J_{11N}^* + J_{11p}^*, \quad (26e)$$
$$E_{11}^* = E_{11N}^* + E_{11p}^*, \quad (26f)$$
$$G_{11}^* = G_{11N}^* + G_{11p}^*, \quad (26g)$$

and

$$\left(A_{ijN}, B_{ijN}, D_{ijN}\right) = \int_{-h_N}^{h_N} C_{ijN}(1, z, z^2)\, dz, \quad (27a)$$
$$\left(A_{ijp}, B_{ijp}, D_{ijp}\right) = \int_{h_N}^{h_N+h_p} C_{ijp}(1, z, z^2)\, dz,$$
$$\left(N_{xp}, N_{\theta p}\right) = \int_{h_N}^{h_N+h_p}\left(e_{31p}, e_{32p}\right)\bar{E}_{zp}\, dz + \quad (27b)$$
$$\left(e_{31p}^s, e_{32p}^s\right)\bar{E}_{zp},$$
$$\left(M_{xp}, M_{\theta p}\right) = \int_{h_N}^{h_N+h_p}\left(e_{31p}, e_{32p}\right)\bar{E}_{zp}\, z dz \quad (27c)$$
$$+\left(e_{31p}^s, e_{32p}^s\right)\bar{E}_{zp}\left(h_N + h_p\right),$$

$$A_{11}^* = A_{22}^* = (\lambda^{s_1} + 2\mu^{s_1}) + (\lambda^{s_2} + 2\mu^{s_2}) \quad (27d)$$
$$A_{12}^* = A_{21}^* = \left(\tau_0^{s_1} + \lambda^{s_1}\right) + \left(\tau_0^{s_2} + \lambda^{s_2}\right),$$
$$A_{66}^* = \left(\mu^{s_1} - (\tau_0^{s_1}/2)\right) + \left(\mu^{s_2} - (\tau_0^{s_2}/2)\right),$$
$$B_{11}^* = B_{22}^* = (\lambda^{s_2} + 2\mu^{s_2})\left(h_N + h_p\right) \quad (27e)$$
$$-(\lambda^{s_1} + 2\mu^{s_1})(h_N), B_{12}^* = B_{21}^* = \left(\tau_0^{s_2} + \lambda^{s_2}\right) \times$$
$$\left(h_N + h_p\right) - \left(\tau_0^{s_1} + \lambda^{s_1}\right)(h_N),$$
$$B_{66}^* = \left(\mu^{s_2} - (\tau_0^{s_2}/2)\right)\left(h_N + h_p\right) -$$
$$\left(\mu^{s_1} - (\tau_0^{s_1}/2)\right)(h_N),$$
$$D_{11}^* = D_{22}^* = (\lambda^{s_2} + 2\mu^{s_2})\left(h_N + h_p\right)^2 \quad (27f)$$
$$+(\lambda^{s_1} + 2\mu^{s_1})(h_N)^2, D_{12}^* = D_{21}^* = \left(\tau_0^{s_2} + \lambda^{s_2}\right) \times$$
$$\left(h_N + h_p\right)^2 + \left(\tau_0^{s_1} + \lambda^{s_1}\right)(h_N)^2,$$
$$D_{66}^* = \left(\mu^{s_2} - (\tau_0^{s_2}/2)\right)\left(h_N + h_p\right)^2 +$$
$$\left(\mu^{s_1} - (\tau_0^{s_1}/2)\right)(h_N)^2,$$

$$F_{11N}^* = \int_{-h_N}^{h_N} \frac{\upsilon_N\left(\frac{\left(\tau_0^{s_2} - \tau_0^{s_1}\right)}{2} + \frac{\left(\tau_0^{s_2} + \tau_0^{s_1}\right)z}{2h_N + h_p}\right)}{(1-\upsilon_N)} dz, \quad (27g)$$

$$F_{11p}^* = \int_{h_N}^{h_N+h_p} \frac{\upsilon_p\left(\frac{\left(\tau_0^{s_2} - \tau_0^{s_1}\right)}{2} + \frac{\left(\tau_0^{s_2} + \tau_0^{s_1}\right)z}{2h_N + h_p}\right)}{(1-\upsilon_p)} dz,$$

$$J_{11N}^* = \int_{-h_N}^{h_N} \frac{\upsilon_N\left(\frac{(\rho^{s_1} - \rho^{s_2})}{2} - \frac{(\rho^{s_1} + \rho^{s_2})z}{2h_N + h_p}\right)}{(1-\upsilon_N)} dz, \quad (27h)$$

$$J_{11p}^* = \int_{h_N}^{h_N+h_p} \frac{\upsilon_p\left(\frac{(\rho^{s_1} - \rho^{s_2})}{2} - \frac{(\rho^{s_1} + \rho^{s_2})z}{2h_N + h_p}\right)}{(1-\upsilon_p)} dz,$$

$$E_{11N}^* = \int_{-h_N}^{h_N} \frac{\upsilon_N\left(\frac{\left(\tau_0^{s_2} - \tau_0^{s_1}\right)z}{2} + \frac{\left(\tau_0^{s_2} + \tau_0^{s_1}\right)z^2}{2h_N + h_p}\right)}{(1-\upsilon_N)} dz, \quad (27i)$$

$$E_{11p}^* = \int_{h_N}^{h_N+h_p} \frac{\upsilon_p\left(\frac{\left(\tau_0^{s_2} - \tau_0^{s_1}\right)z}{2} + \frac{\left(\tau_0^{s_2} + \tau_0^{s_1}\right)z^2}{2h_N + h_p}\right)}{(1-\upsilon_p)} dz,$$

$$G_{11N}^* = \int_{-h_N}^{h_N} \frac{\upsilon_N\left(\frac{(\rho^{s_1} - \rho^{s_2})z}{2} - \frac{(\rho^{s_1} + \rho^{s_2})z^2}{2h_N + h_p}\right)}{(1-\upsilon_N)} dz, \quad (27j)$$

$$G_{11p}^* = \int_{h_N}^{h_N+h_p} \frac{\upsilon_p\left(\frac{(\rho^{s_1} - \rho^{s_2})z}{2} - \frac{(\rho^{s_1} + \rho^{s_2})z^2}{2h_N + h_p}\right)}{(1-\upsilon_p)} dz,$$

Note that, because of geometric symmetry, the expressions B_{ijN} is zero, i.e. $\left(B_{ijN} = 0\right)$.

The equations of motion and corresponding boundary conditions of the piezoelectric shell can be derived from Hamilton's principle

$$\int_0^t \left(\delta T - \delta\pi + \delta w_f\right) dt = 0, \quad (28)$$

and by taking the variations of displacements u, v and w, and then integrating by parts, and by equating the coefficients of δu ،δv and δw to zero, the governing equations of motion are derived as [29]:

$$\delta u: \quad \frac{\partial N_{xx}}{\partial x} + \frac{1}{R}\frac{\partial N_{x\theta}}{\partial \theta} = I\frac{\partial^2 u}{\partial t^2}, \quad (29)$$

$$\delta v: \quad \frac{\partial N_{x\theta}}{\partial x} + \frac{1}{R}\frac{\partial N_{\theta\theta}}{\partial \theta} = I\frac{\partial^2 v}{\partial t^2}, \quad (30)$$

$$\delta w: \quad \frac{\partial^2 M_{xx}}{\partial x^2} + \frac{2}{R}\frac{\partial^2 M_{x\theta}}{\partial x \partial \theta} + \frac{1}{R^2}\frac{\partial^2 M_{\theta\theta}}{\partial \theta^2} \quad (31)$$
$$-\frac{N_{\theta\theta}}{R} + N_{xx}\frac{\partial^2 w}{\partial x^2} + \frac{\partial N_{xx}}{\partial x}\frac{\partial w}{\partial x} + \frac{N_{\theta\theta}}{R^2}\frac{\partial^2 w}{\partial \theta^2} + \frac{1}{R^2}\frac{\partial N_{\theta\theta}}{\partial \theta}\frac{\partial w}{\partial \theta} +$$
$$\frac{2}{R}N_{x\theta}\frac{\partial^2 w}{\partial x \partial \theta} + \frac{1}{R}\frac{\partial N_{x\theta}}{\partial x}\frac{\partial w}{\partial \theta} + \frac{1}{R}\frac{\partial N_{x\theta}}{\partial \theta}\frac{\partial w}{\partial x} = I\frac{\partial^2 w}{\partial t^2} - f cos\omega t,$$

and boundary conditions are obtained as follows:

$$\delta u = 0 \quad or \quad N_{xx}n_x + \frac{1}{R}N_{x\theta}n_\theta = 0, \quad (32a)$$

$$\delta v = 0 \quad or \quad N_{x\theta}n_x + \frac{1}{R}N_{\theta\theta}n_\theta = 0, \quad (32b)$$

$$\delta w = 0 \quad or \quad \left(\frac{\partial M_{xx}}{\partial x} + \frac{1}{R}\frac{\partial M_{x\theta}}{\partial \theta} + N_{xx}\frac{\partial w}{\partial x} + \frac{N_{x\theta}}{R}\frac{\partial w}{\partial \theta}\right)n_x \quad (32c)$$
$$+\left(\frac{1}{R}\frac{\partial M_{x\theta}}{\partial x} + \frac{1}{R^2}\frac{\partial M_{\theta\theta}}{\partial \theta} + \frac{N_{x\theta}}{R}\frac{\partial w}{\partial x} + \frac{N_{\theta\theta}}{R^2}\frac{\partial w}{\partial \theta}\right)n_\theta = 0, \quad (32d)$$

$$\frac{\partial w}{\partial x} = 0 \quad or \quad M_{xx}n_x + \frac{1}{R}M_{x\theta}n_\theta = 0\,, \quad (32e)$$

$$\frac{\partial w}{\partial \theta} = 0 \quad or \quad \frac{1}{R}M_{x\theta}n_x + \frac{1}{R^2}M_{\theta\theta}n_\theta = 0, \quad (32d)$$

But in order to solve the problem explicitly and more easily, and the direct use of boundary conditions in equations, the assumed mode method will be used. After substituting Eqs. (27) into strain and kinetic energies Eqs. (20) and (21) and using following dimensionless parameters

$$\bar{u} = \frac{u}{h_N}, \bar{v} = \frac{v}{h_N}, \bar{w} = \frac{w}{h_N}, \xi = \frac{x}{L}, \bar{b} = \frac{b}{h_N}, \quad (33)$$
$$\bar{A}_{ijN} = \frac{A_{ijN}}{A_{11N}}, \bar{B}_{ijN} = \frac{B_{ijN}}{A_{11N}h_N}, \bar{D}_{ijN} = \frac{D_{ijN}}{A_{11N}h_N^2},$$
$$\bar{A}_{ijp} = \frac{A_{ijp}}{A_{11N}}, \bar{A}_{ij}^* = \frac{A_{ij}^*}{A_{11N}}, \bar{B}_{ijp} = \frac{B_{ijp}}{A_{11N}h_N},$$
$$\bar{B}_{ij}^* = \frac{B_{ij}^*}{A_{11N}h_N}, \bar{D}_{ijp} = \frac{D_{ijp}}{A_{11N}h_N^2}, \bar{D}_{ij}^* = \frac{D_{ij}^*}{A_{11N}h_N^2},$$
$$\bar{F}_{11N}^* = \frac{F_{11N}^*}{A_{11N}h_N}, \bar{F}_{11p}^* = \frac{F_{11p}^*}{A_{11N}h_N}, \bar{E}_{11N}^* = \frac{E_{11N}^*}{A_{11N}h_N^2},$$
$$\bar{E}_{11p}^* = \frac{E_{11p}^*}{A_{11N}h_N^2}, \bar{J}_{11N}^* = \frac{J_{11N}^*}{\rho_N h_N^2}, J_{11p}^* = \frac{J_{11p}^*}{\rho_N h_N^2},$$
$$\bar{G}_{11N}^* = \frac{G_{11N}^*}{\rho_N h_N^3}, G_{11p}^* = \frac{G_{11p}^*}{\rho_N h_N^3}, \bar{N}_{xp}^* = \frac{N_{xp}^*}{A_{11N}},$$
$$\bar{N}_{\theta p}^* = \frac{N_{\theta p}^*}{A_{11N}}, \bar{M}_{xp}^* = \frac{M_{xp}^*}{A_{11N}h_N}, \bar{M}_{\theta p}^* = \frac{M_{\theta p}^*}{A_{11N}h_N},$$
$$\bar{\tau}_0^s = \frac{\tau_0^s}{A_{11N}}, m_0 = \frac{L}{R}, m_1 = \frac{L}{h_N}, m_2 = \frac{h_N}{R} = \frac{1}{\bar{R}},$$
$$\bar{h}_p = \frac{h_p}{R}, m_3 = \frac{I}{2\rho_N h_N}, m_4 = \frac{h_p}{h_N}, \tau = \hat{\Omega}t,$$
$$\hat{\Omega} = \sqrt{\frac{A_{11N}}{2\rho_N h_N L^2}}, \Omega = \frac{\omega}{\hat{\Omega}}, \bar{F} = \frac{fL^2}{A_{11N}m_3 h_N{}^2},$$

Respectively, strain and kinetic energies and are obtained as follows:

$$\pi = \frac{1}{2}\int_0^L \int_0^{2\pi} \left\{\alpha_1\left(\frac{\partial \bar{u}}{\partial \xi}\right)^2 + \alpha_2\left(\frac{\partial \bar{u}}{\partial \theta}\right)^2 \frac{\partial \bar{v}}{\partial \theta} + \alpha_3\frac{\partial \bar{u}}{\partial \xi} + \right. \quad (34)$$
$$\alpha_4\frac{\partial \bar{v}}{\partial \xi}\frac{\partial \bar{u}}{\partial \theta} + \alpha_5\bar{w}\frac{\partial \bar{u}}{\partial \xi} + \alpha_6\frac{\partial \bar{u}}{\partial \xi}\left(\frac{\partial \bar{w}}{\partial \xi}\right)^2 + \alpha_7\frac{\partial \bar{u}}{\partial \xi}\left(\frac{\partial \bar{w}}{\partial \theta}\right)^2 +$$
$$\alpha_8\frac{\partial \bar{u}}{\partial \theta}\frac{\partial \bar{w}}{\partial \xi}\frac{\partial \bar{w}}{\partial \theta} + \alpha_9\left(\frac{\partial \bar{v}}{\partial \theta}\right)^2 + \alpha_{10}\frac{\partial \bar{v}}{\partial \theta}\left(\frac{\partial \bar{w}}{\partial \theta}\right)^2 +$$

$$\alpha_{11}\frac{\partial\bar{v}}{\partial\theta}\left(\frac{\partial\bar{w}}{\partial\xi}\right)^2+\alpha_{12}\bar{w}\frac{\partial\bar{v}}{\partial\theta}+\alpha_{13}\left(\frac{\partial\bar{v}}{\partial\xi}\right)^2+\alpha_{14}\frac{\partial\bar{v}}{\partial\xi}\frac{\partial\bar{w}}{\partial\xi}\frac{\partial\bar{w}}{\partial\theta}+$$
$$\alpha_{15}\bar{w}^2+\alpha_{16}\left(\frac{\partial\bar{w}}{\partial\xi}\right)^4+\alpha_{17}\left(\frac{\partial\bar{w}}{\partial\theta}\right)^4+$$
$$+\alpha_{18}\left(\frac{\partial\bar{w}}{\partial\xi}\right)^2\left(\frac{\partial\bar{w}}{\partial\theta}\right)^2+\alpha_{19}\bar{w}\left(\frac{\partial\bar{w}}{\partial\xi}\right)^2+\alpha_{20}\bar{w}\left(\frac{\partial\bar{w}}{\partial\theta}\right)^2+$$
$$\alpha_{21}\frac{\partial\bar{u}}{\partial\theta}\frac{\partial^2\bar{w}}{\partial\xi\partial\theta}+\alpha_{22}\frac{\partial\bar{u}}{\partial\xi}\frac{\partial^2\bar{w}}{\partial\theta^2}+\alpha_{23}\frac{\partial\bar{u}}{\partial\xi}\frac{\partial^2\bar{w}}{\partial\xi^2}+\alpha_{24}\frac{\partial\bar{v}}{\partial\theta}\frac{\partial^2\bar{w}}{\partial\xi^2}+$$
$$+\alpha_{25}\frac{\partial\bar{v}}{\partial\xi}\frac{\partial^2\bar{w}}{\partial\xi\partial\theta}+\alpha_{26}\frac{\partial\bar{v}}{\partial\theta}\frac{\partial^2\bar{w}}{\partial\theta^2}+\alpha_{27}\frac{\partial^2\bar{w}}{\partial\xi^2}\left(\frac{\partial\bar{w}}{\partial\theta}\right)^2+$$
$$\alpha_{28}\bar{w}\frac{\partial^2\bar{w}}{\partial\xi^2}+\alpha_{29}\frac{\partial^2\bar{w}}{\partial\theta^2}\left(\frac{\partial\bar{w}}{\partial\xi}\right)^2+\alpha_{30}\frac{\partial^2\bar{w}}{\partial\xi^2}\left(\frac{\partial\bar{w}}{\partial\xi}\right)^2+$$
$$\alpha_{31}\frac{\partial^2\bar{w}}{\partial\theta^2}\left(\frac{\partial\bar{w}}{\partial\theta}\right)^2+\alpha_{32}\frac{\partial^2\bar{w}}{\partial\xi\partial\theta}\frac{\partial\bar{w}}{\partial\xi}\frac{\partial\bar{w}}{\partial\theta}+\alpha_{33}\bar{w}\frac{\partial^2\bar{w}}{\partial\theta^2}+$$
$$\alpha_{34}\left(\frac{\partial^2\bar{w}}{\partial\xi^2}\right)^2+\alpha_{35}\left(\frac{\partial^2\bar{w}}{\partial\theta^2}\right)^2+\alpha_{36}\left(\frac{\partial^2\bar{w}}{\partial\xi\partial\theta}\right)^2+$$
$$\alpha_{37}\frac{\partial^2\bar{w}}{\partial\xi^2}\frac{\partial^2\bar{w}}{\partial\theta^2}+\alpha_{38}\bar{w}+\alpha_{39}\frac{\partial\bar{u}}{\partial\xi}+\alpha_{40}\frac{\partial\bar{v}}{\partial\theta}+$$
$$\alpha_{41}\left(\frac{\partial\bar{w}}{\partial\xi}\right)^2+\alpha_{43}\frac{\partial^2\bar{w}}{\partial\xi^2}+\alpha_{44}\frac{\partial^2\bar{w}}{\partial\theta^2}+\alpha_{45}\frac{\partial^2\bar{w}}{\partial\xi^2}\frac{\partial^2\bar{w}}{\partial\tau^2}+$$
$$\alpha_{46}\frac{\partial^2\bar{w}}{\partial\theta^2}\frac{\partial^2\bar{w}}{\partial\tau^2}+\alpha_{47}\frac{\partial\bar{u}}{\partial\xi}\frac{\partial^2\bar{w}}{\partial\tau^2}+\alpha_{48}\frac{\partial\bar{v}}{\partial\theta}\frac{\partial^2\bar{w}}{\partial\tau^2}+\alpha_{49}\bar{w}\frac{\partial^2\bar{w}}{\partial\tau^2}+$$
$$\alpha_{50}\left(\frac{\partial\bar{w}}{\partial\xi}\right)^2\frac{\partial^2\bar{w}}{\partial\tau^2}+\alpha_{51}\left(\frac{\partial\bar{w}}{\partial\theta}\right)^2\frac{\partial^2\bar{w}}{\partial\tau^2}+\eta_{33}\bar{E}_{zp}^2h_p\Big\}d\theta dx,$$

$$T=\frac{1}{2}\int_0^L\int_0^{2\pi}\left(\left(\frac{\partial\bar{u}}{\partial\tau}\right)^2+\left(\frac{\partial\bar{v}}{\partial\tau}\right)^2+\left(\frac{\partial\bar{w}}{\partial\tau}\right)^2\right)d\theta dx, \quad (35)$$

$$W_f=\int_0^L\int_0^{2\pi}(\bar{F}cos\Omega\tau)\,\bar{w}d\theta d\xi, \quad (36)$$

$$W_p=\frac{1}{2}\int_0^L\int_0^{2\pi}\begin{pmatrix}\bar{N}_{xp}\left(\frac{\partial\bar{w}}{\partial\xi}\right)^2+\\ m_0^2\bar{N}_{\theta p}\left(\frac{\partial\bar{w}}{\partial\theta}\right)^2\end{pmatrix}d\theta dx, \quad (37)$$

where coefficients of $\alpha_k(k=1..51)$ are introduced in Appendix 1.

5. NONLINEAR VIBRATION ANALYSIS

The assumed mode method is used for changing the partial differential equations into ordinary differential equations. By applying the assumed mode method, the in-plane, transverse and shear deformations can be expressed as general coordinates and mode shape functions that satisfy the geometric boundary conditions, as follows [31]:

$$u(x,\theta,t)=\sum_{m=1}^{M_2}u_{m,0}(\tau)\chi_{mn}(\xi)+ \quad (38a)$$
$$\sum_{m=1}^{M_1}\sum_{n=1}^{N}\begin{bmatrix}u_{m,n,c}(\tau)\,cos(n\theta)\\+u_{m,n,s}(\tau)\,sin(n\theta)\end{bmatrix}\chi_{mn}(\xi)=$$
$$\sum_{i=1}^{M_2+M_1\times N}u_i(\tau)\chi_i(\xi)\vartheta_i(\theta),$$

$$v(x,\theta,t)=\sum_{m=1}^{M_2}v_{m,0}(\tau)\phi_{mn}(\xi)+ \quad (38b)$$
$$\sum_{m=1}^{M_1}\sum_{n=1}^{N}\begin{bmatrix}v_{m,n,c}(\tau)\,sin(n\theta)\\+v_{m,n,s}(\tau)\,cos(n\theta)\end{bmatrix}\phi_{mn}(\xi)=$$
$$\sum_{r=1}^{M_2+M_1\times N}v_r(\tau)\phi_r(\xi)\alpha_r(\theta),$$

$$w(x,\theta,t)=\sum_{m=1}^{M_2}w_{m,0}(\tau)\beta_{mn}(\xi)+ \quad (38c)$$
$$+\sum_{m=1}^{M_1}\sum_{n=1}^{N}\begin{bmatrix}w_{m,n,c}(\tau)\,cos(n\theta)\\+w_{m,n,s}(\tau)\,sin(n\theta)\end{bmatrix}\beta_{mn}(\xi)=$$
$$\sum_{s=1}^{M_2+M_1\times N}w_s(\tau)\beta_s(\xi)\psi_s(\theta),$$

where $\chi_i(\xi)$, $\phi_r(\xi)$ and $\beta_s(\xi)$ are modal functions which satisfy the required geometric boundary conditions. $u_i(\tau)$, $v_r(\tau)$ and $w_s(\tau)$ are unknown functions of time and are related to dynamical response. Substituting Eqs. (38) into Eqs. (34) and (35) and applying the Lagrange equations results in the following reduced-order model of the system:

$$[(M)_u^u]\{\ddot{\bar{u}}\}+[(M)_u^w]\{\ddot{\bar{w}}\}+[(K)_u^u]\{\bar{u}\}+ \quad (39)$$
$$[(K)_u^v]\{\bar{v}\}+[(K)_u^w]\{\bar{w}\}+[(NL)_u^w]\{\bar{w}^2\}=\left[\bar{F}_{up}\right],$$
$$[(M)_v^v]\{\ddot{\bar{v}}\}+[(M)_v^w]\{\ddot{\bar{w}}\}+[(K)_v^u]\{\bar{u}\}+ \quad (40)$$
$$[(K)_v^v]\{\bar{v}\}+[(K)_v^w]\{\bar{w}\}+[(NL)_v^w]\{\bar{w}^2\}=\left[\bar{F}_{vp}\right],$$
$$\left[(M)_w^w+(K)_{w2}^{\ddot{w}}\{\bar{w}\}\right]\{\ddot{\bar{w}}\}+[(K)_w^u]\{\bar{u}\}+ \quad (41)$$
$$[(K)_w^v]\{\bar{v}\}+[(K)_w^w]\{\bar{w}\}+[(NL)_w^u]\{\bar{w}\bar{u}\}+$$
$$[(NL)_w^v]\{\bar{w}\bar{v}\}[(NL)_{w2}^w]\{\bar{w}^2\}+[(NL)_{w3}^w]\{\bar{w}^3\}=$$
$$\left[\bar{F}_{wp}\right]+[\bar{F}_H cos\Omega\tau],$$

where (M), (K) and (NL) are mass, stiffness and the nonlinear stiffness matrixes. Also, $\bar{F}_u$, $\bar{F}_v$ and $\bar{F}_w$ are applied loads by piezoelectric voltage and surface stress. All coefficients of mass, stiffness, nonlinear term matrixes and applied loads Eqs. (39)- (41) are presented in Appendix 2.

Figure 2(a-c) represent the nonlinear dynamic (the steady state) response of the FG-PCNS with the material and geometrical parameters Tables 1-3 and by ode45 solver. It can be seen from Figure 2 that the effect of the axial and circumferential inertia terms is so small in comparison with the transverse inertia term that one can ignore it in Eqs. (39) and (40) under an admissive precision. Afterwards, it is feasible from Eqs, (39) and (40) to solve the unknown functions $u_{ij}(\tau)$ and $v_{kl}(\tau)$ in terms of $w_{op}(\tau)$ and by substituting the results into Eq. (41), one can obtain the nonlinear differential equation of transverse motion as

$$\begin{Bmatrix}(M)_w^w+\begin{bmatrix}(\widehat{M})_u^{wu}\\(\widehat{M})_v^{wv}\end{bmatrix}+\\ \left(\begin{bmatrix}(K)_{w2}^{\ddot{w}}\end{bmatrix}-[(NL)_w^u]\left(\widehat{M}\right)_u^w\right)\{\bar{w}\}\\ -[(NL)_w^v]\left(\widehat{M}\right)_v^w\end{Bmatrix}\{\ddot{\bar{w}}\}+ \quad (42)$$
$$\left\{(K)_w^w+\begin{bmatrix}(\widehat{K})_u^{wu}\\(\widehat{K})_v^{wv}\end{bmatrix}+[(NL)_w^u]\hat{F}_{up}+[(NL)_w^v]\hat{F}_{vp}\right\}\{\bar{w}\}$$
$$+\left\{\begin{bmatrix}(\widehat{NL})_u^{wu}\\(\widehat{NL})_v^{wv}\end{bmatrix}-[(NL)_w^u]\left(\widehat{K}\right)_u^w-\right\}\{\bar{w}^2\}+$$
$$\left\{\begin{matrix}-[(NL)_w^u]\left(\widehat{NL}\right)_u^w-[(NL)_w^v]\left(\widehat{NL}\right)_v^w\\+[(NL)_{w3}^w]\end{matrix}\right\}\{\bar{w}^3\}+$$
$$\begin{bmatrix}\hat{F}_{wup}\\\hat{F}_{wvp}\end{bmatrix}=\bar{F}_{wp}+\bar{F}_H cos\Omega\tau,$$

where the all coefficients of Equation (42), i.e.: $(\widehat{M})_u^w, (\widehat{M})_v^w, (\widehat{M})_u^{wu}, (\widehat{M})_v^{wv}, (\widehat{K})_u^w, (\widehat{K})_v^w, (\widehat{K})_u^{wu}, (\widehat{K})_v^{wv}, (\widehat{NL})_u^w, (\widehat{NL})_v^w, (\widehat{NL})_u^{wu}, (\widehat{NL})_v^{wv}, \hat{F}_{up}, \hat{F}_{vp}, \hat{F}_{wup}, \hat{F}_{wvp}$, are presented in the Appendix 3.

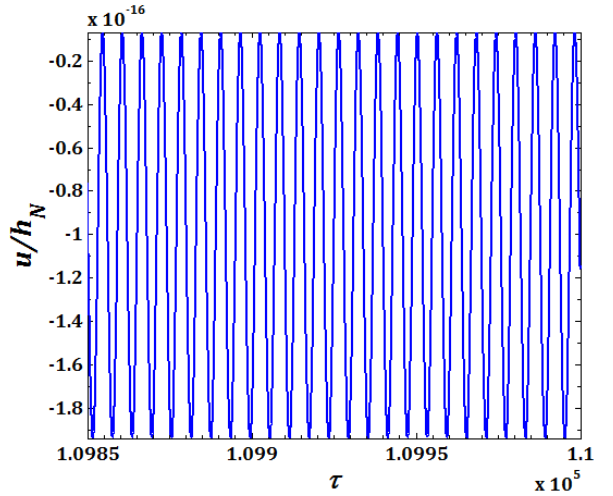

(a) Axial direction u

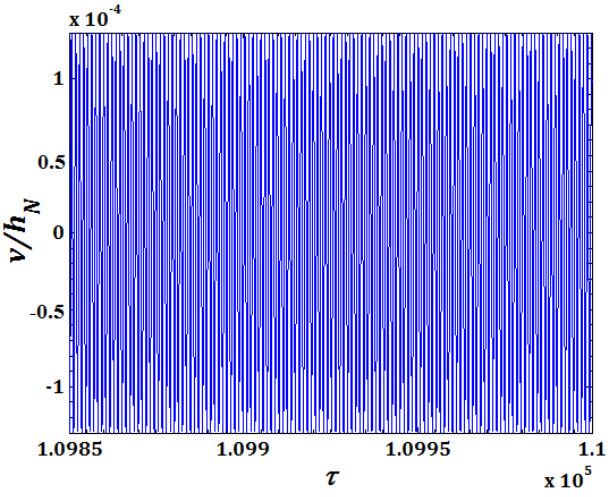

(b) Tangential direction v

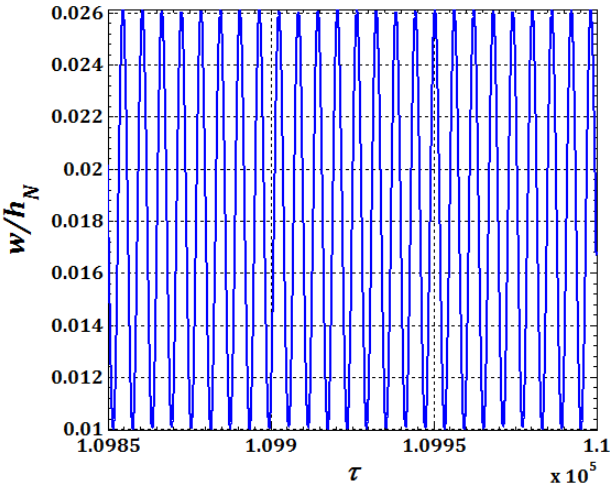

(c) Radial direction w

Figure 2. The nonlinear dynamic response of the SS nano resonator in three directions

From Eq. (42) the fundamental natural frequencies of vibration of the FG-PCNS can be determined by the relation

$$\omega_n = \sqrt{\frac{\left[(K)_w^w + \begin{bmatrix}(\hat{K})_u^{wu}\\(\hat{K})_v^{wv}\end{bmatrix} + [(NL)_w^u]\hat{F}_{up} + [(NL)_w^v]\hat{F}_{vp}\right]}{\left[(M)_w^w + \begin{bmatrix}(\hat{M})_u^{wu}\\(\hat{M})_v^{wv}\end{bmatrix}\right]}}, \qquad (43)$$

6. RESULTS AND DISCUSSIONS

In this section, first, the surface energy effect on the free and linear vibration analysis of a piezoelectric cylindrical nano-shell is investigated. In order to simplify the presentation, C-C, S-S, C-S and C-F represent clamped edge, simply supported edge, clamped-simply supported edge and clamped-free edge, respectively. Then the nonlinear dynamic (the steady state) response of the forced and nonlinear equations of FG-PCNS is solved by *ode45 solver* of MATLAB (numerical simulation). At the end, nonlinear dynamic response analysis is investigated by the complex-averaging method and solved by the arc-length continuation method (semi-analytical method), which has a periodic behavior at some of the nanoresonator stimulation frequencies. The nonhomogeneous nano-shell considered in the following examples is composed of stainless steel and nickel and the nonhomogeneous distribution of properties in the thickness direction is varied according to the volume fraction power-law function. The material properties for stainless steel and nickel are shown in Table 1 [33].

Table 1. Properties of stainless steel and nickel [33]

Stainless steel		
$E_B(Nm^{-2})$	υ_B	$\rho_B(kg\ m^{-3})$
2.08×10^{11}	0.381	8166
Nichel		
$E_T(Nm^{-2})$	υ_T	$\rho_T(kg\ m^{-3})$
2.05×10^{11}	0.31	8900

The piezoelectric layer is assumed to be made of PZT-4 material, and the properties of PZT-4 are given in Table 2 [33]. Also, the material and geometrical parameters used in all following results are shown in Table 3 [19, 34].

Table 2. Properties of PZT-4 [33]

$E_p(Gpa)$	υ_p	$e_{31p}(C/m^2)$
95	0.3	-5.2
$e_{32p}(C/m^2)$	$\eta_{33p}(10^{-11}\ F/m)$	$\rho_p(kg\ m^{-3})$
-5.2	560	7500

Table 3. The material and geometrical parameters

$R(m)$	L/R	h_N/R
1×10^{-9}	10	0.01
h_p/R	$\lambda^{s_1}(N/m)$	$\mu^{s_1}(N/m)$
0.01	0.1	0.05
$\tau_0^{s_1}\ (N/m)$	$\rho^{s_1}(kg/m^2)$	$V_p(V)$
5.5×10^{-3}	3.17×10^{-7}	1×10^{-5}
$\lambda^{s_2}(N/m)$	$\mu^{s_2}(N/m)$	$\tau_0^{s_2}(N/m)$
0.1	0.05	5.5×10^{-3}
$e_{31p}^{s_2}(C/m)$	$e_{32p}^{s_2}(C/m)$	$\rho^{s_2}(kg/m^2)$
-3×10^{-8}	-3×10^{-8}	5.61×10^{-6}
$F(N)$		
5×10^{-5}		

Of course, the geometrical parameters can be varying according to the type of problem. In this paper, the results are presented in dimensionless form and thus the results are not limited to a particular type of matter. The data presented in the form of sample data to approximate the numbers used in the actual range.

6.1. Convergence and comparison studies

In this subsection, a few well-studied classical and some nonclassical boundary conditions frequently encountered in practice are taken as calculation examples. The method proposed in this paper is validated by comparing the present numerical results with previously published in the literature. If we neglect the piezoelectric and surface effects, the present model can be reduced to the macroscopic cylindrical shell model.

The dimensionless natural frequencies ($\omega_n = \widehat{\Omega}R\sqrt{(1-\upsilon^2)\rho/E}$) of macroscopic cylindrical shell are listed the three classical boundary conditions are presented in Table 4 together with those previously given by Loy et al. [28]. The parameters used in this example are: $m = 1,\ L/R = 20,\ h_N/R = 0.01$, and $\upsilon = 0.3$. It can be observed from Table 3 that the present results agree very well with the reference solutions, which indicates that the method presented in this paper is suitable and of high accuracy for free vibration analysis of cylindrical shells with classical boundary conditions. The slight differences in the results may be attributed to the different shell theories and solution approaches adopted in the literature and in this paper.

In table 5, the convergence criterion of the present method is examined for the four boundary conditions S-S, S-C, C-C and C-F for dimensionless natural frequencies. It is observed from these table that as the number, N, the Ritz polynomial functions is increased, the convergence is achieved rapidly. It is also seen that convergence of the method is influenced by the type of boundary conditions used.

Table 4. Comparison of dimensionless natural frequencies ω_n for S-S, S-C and C-C boundary conditions of a homogeneous cylindrical shell

n	S-S	
	Present	Loy et al.[28]
1	0.016126	0.016101
2	0.005225	0.009382
3	0.021753	0.022105
4	0.034303	0.042095
n	S-C	
	Present	Loy et al.[28]
1	0.023299	0.023974
2	0.010963	0.011225
3	0.018553	0.022310
4	0.036300	0.042139
n	C-C	
	Present	Loy et al.[28]
1	0.034074	0.032885
2	0.014202	0.013932
3	0.018713	0.022672
4	0.041386	0.042208

Table 5. Convergence of dimensionless natural frequencies ω_n for S-S, S-C, C-C and C-F piezoelectric cylindrical shell

	S-S		
n	$N = 1$	$N = 3$	$N = 5$
0	0.16459	0.16459	0.16459
1	0.12762	0.12762	0.12762
2	0.13966	0.13966	0.13966
3	0.25244	0.25244	0.25244
	C-C		
n	$N = 1$	$N = 3$	$N = 5$
0	0.16459	0.16459	0.16459
1	0.41303	0.06910	0.05963
2	0.55925	0.13155	0.13067
3	0.67239	0.24995	0.24973
	S-C		
n	$N = 1$	$N = 3$	$N = 5$
0	0.16459	0.16459	0.16459
1	0.41303	0.06910	0.05963
2	0.55925	0.13155	0.13067
3	0.67239	0.24995	0.24973
	C-F		
n	$N = 1$	$N = 3$	$N = 5$
0	0.16459	0.16459	0.16459
1	0.41303	0.06910	0.05963
2	0.55925	0.13155	0.13067
3	0.67239	0.24995	0.24973

6.2. Parametric study for natural frequency and time response solutions

The accuracy of the present study was verified in the previous section. Here, some numerical results are

presented to explore the effects of involved parameters on the vibration behavior of cylindrical piezoelectric nano-shell. Also, all following results are investigated in the value of mode number $m = 3$ and $n = 1$. According to Eq. 38, the number of natural frequency for mode number $(m, n) = (3,1)$ is $(2n + 1) \times m = 9$; i.e. nine (9) natural frequency has in this mode number which consider first, two,…, nine natural frequency ω_i $(i = 1..9)$.

Figures 3 and 4, respectively illustrates the effect of different boundary conditions (S-S, C-C, C-S and C-F) on dimensi8onless natural frequencies ω_n and the nonlinear dynamic response of the piezoelectric nano-shell versus length-to-small radius ratio (L/R).

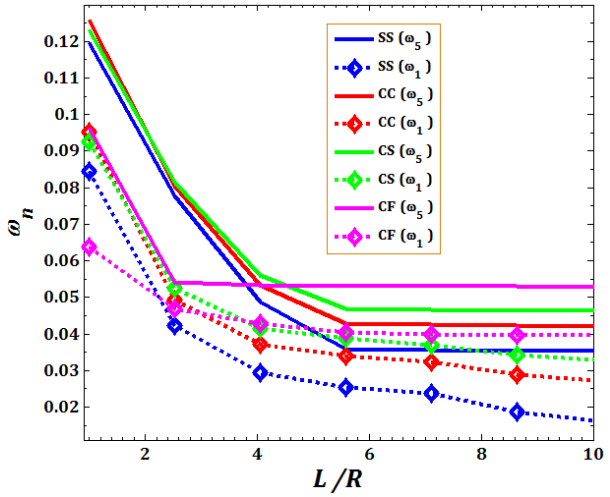

Figure 3. The effect of L/R ratio on ω_n of FG-PCNS for different boundary condition

From Figure 3, it can be seen that for all boundary conditions, the fundamental frequency decreases with the increase of the L/R ratio. In addition, the length-to-small radius ratio of cylindrical shell has an important effect on natural frequency. Note that in this figure (Figure 3), due to the use of all boundary conditions, the results are presented for the first ω_1 and the five ω_5 natural frequencies.

The reason is that a higher L/R ratio lead to a decrease in the nanoshell stiffness, and cause to lower natural frequencies of nanoshell and the vibrational behavior of the shell with the larger L/R ratio is less sensitive to variations of boundary conditions and by increasing this ratio, the frequency also decreases. The nonlinear dynamic (steady state) responses of the piezoelectric nano-shell for different boundary conditions (S-S, C-C, C-S and C-F) are presented in Figure 4 with $L/R = 10$ and considering of primary resonance ω_1.

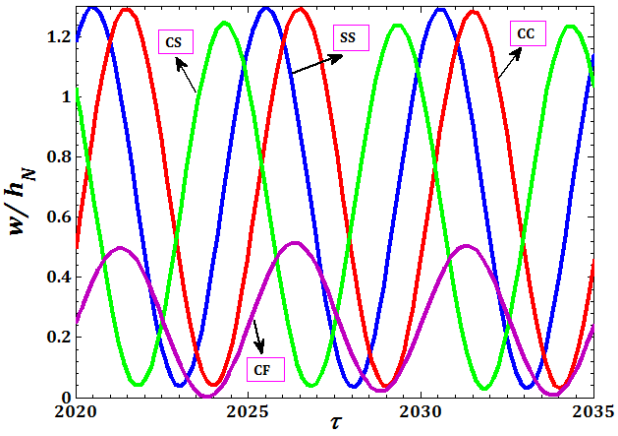

Figure 4. The nonlinear dynamic response of FG-PCNS for different boundary condition

In this following, for investigation of the natural frequencies and the nonlinear dynamic response only S-S boundary condition with surface energy effects is considered.

Figure 5 shows the effects of the ratio thickness L/R on the nonlinear dynamic response of the FG-PCNS in primary resonance ω_1 for four cases $L/R = (3,5,10,20)$. It can be seen, with increasing the length to radius ratio L/R, the oscillation amplitude is less but the number of oscillations increases.

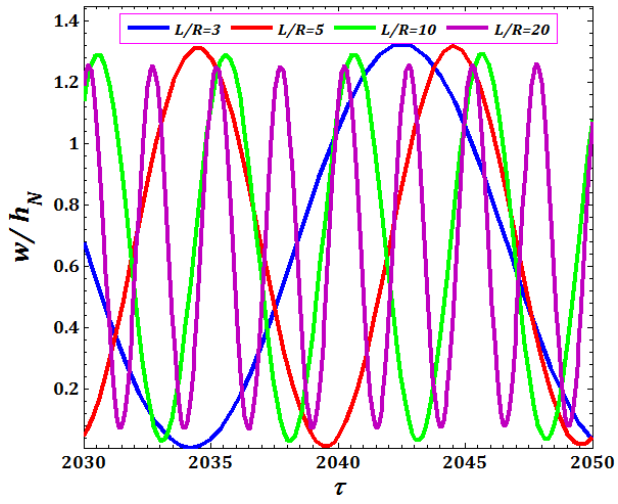

Figure 5. The effects of the L/R ratio on the nonlinear dynamic response of the FG-PCNS

Figure 6 illustrates the effect of shell thickness to small radius ratio h_N/R on dimensionless natural frequencies of the FG-PCNS. It can be seen that by increasing the thickness shell to small radius ratio h_N/R, the natural frequency increases which in the higher ratio h_N/R, increase in the frequencies is more evident. For example, in the ratio of $h_N/R = 0.5$, the frequency ω_7 is more than 8 times the first frequency ω_1.

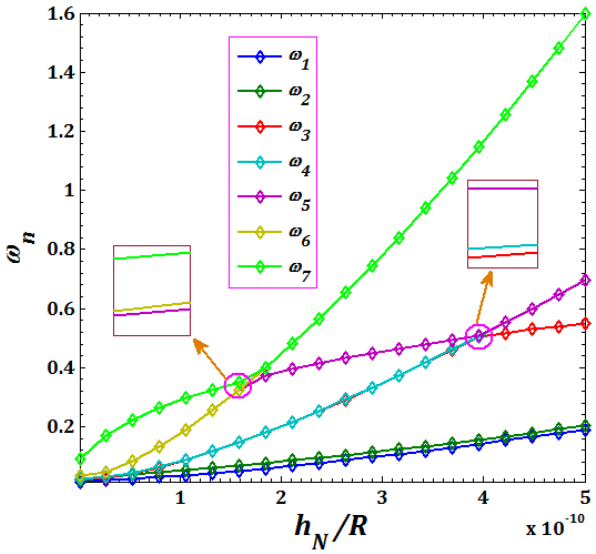

Figure 6. The effect of h_N/R ratio on dimensionless natural frequencies ω_n for SS FG-PCNS

The dimensionless natural frequencies of the FG-PCNS versus piezoelectric thickness to small radius ratio (h_p/R) with surface effects is presented in Figure 7. It can be shown that by increasing the ratio h_p/R, the natural frequency increases which in the higher ratio h_p/R, increase in the frequencies is more evident. For example, in the ratio of $h_p/R = 0.5$, the frequency ω_7 is more than 12 times the first frequency ω_1.

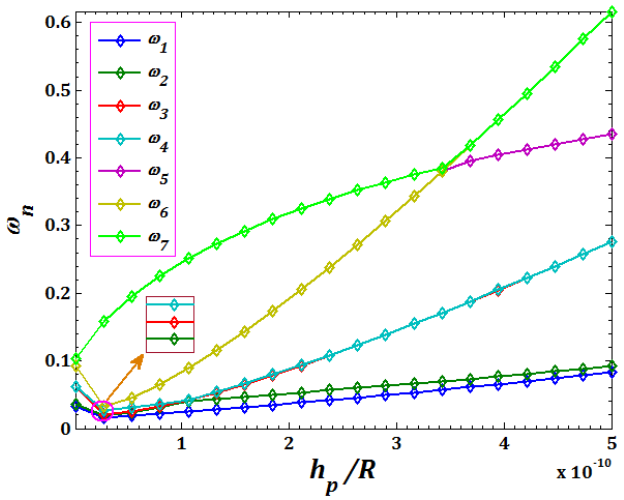

Figure 7. The effect of h_p/R ratio on dimensionless natural frequencies ω_n of FG-PCNS

The influence of excitation force F on the nonlinear dynamic response of the FG-PCNS for SS boundary condition illustrate in Figure 10. From this Figure, it can be seen that when F is increased, the value of the FG-PCNS amplitude increases and vice versa.

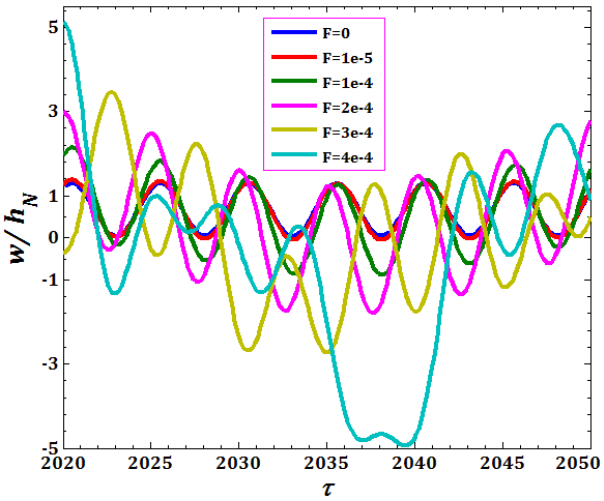

Figure 8. The effect of excitation force F on the nonlinear dynamic response of FG-PCNS

6.3. Analytical solutions

In this section, Complex averaging method combined with arc-length continuation is used to achieve an approximate solution for nonlinear frequency response of FG-PECNS. In order to study the steady state response of the system, the complexification-averaging method is applied [35, 36]. For each mode of the nano shell, new complex variables are introduced in the following equation.

$$\phi = (\dot{\bar{w}} + i\bar{\omega}\bar{w})e^{-i\bar{\omega}\tau} \tag{44}$$

By introducing these new variables, dynamics of system is decomposed into fast and slowly varying terms, where ϕ is the slow term and $\bar{\omega}$ is the fast one. Displacement variables and their derivatives can be expressed in terms of these new complex variables.

$$\bar{w} = \bar{w}_{st} + \frac{\phi e^{i\bar{\omega}\tau} - \phi^* e^{-i\bar{\omega}\tau}}{2i\bar{\omega}}, \tag{45}$$
$$\dot{\bar{w}} = \frac{\phi e^{i\bar{\omega}\tau} + \phi^* e^{-i\bar{\omega}\tau}}{2},$$
$$\ddot{\bar{w}} = \dot{\phi} e^{i\bar{\omega}\tau} + i\bar{\omega}\frac{\phi e^{i\bar{\omega}\tau} - \phi^* e^{-i\bar{\omega}\tau}}{2},$$

where in the above expression, $\bar{w}_{st}$ are the static displacements and subscript * means complex conjugate. By substituting $\bar{w}$ and its derivatives into Eq. (42), a set of complex equations governing the slowly complex amplitude ϕ is obtained. Most methods for solving nonlinear equations of a nonlinear system are iterative, e.g. the continuation methods. These methods are used to compute approximate solutions for nonlinear systems with parameterized nonlinear equations.

6.3.1. Verification and convergence studies

In this sub-section, it is necessary to examine the accuracy of the original equations of motion by numerical simulation. Nonlinear dynamic response (the time response solution) of the equations of FG-PECNS is solved by *ode45 solver* of MATLAB (by Runge-kutta method as numerical simulation) and also, this equation is obtained by the complex-averaging method and solved by the arc-length continuation method (semi-analytical method), which has a periodic behavior at some of the nanoresonator stimulation frequencies. Figure 9 represents the nonlinear dynamic (the steady state) response of the FG-PECNS for fixed values of the system parameters in primary resonance and in modes $(m = 3, n = 1)$ by ode45 solver.

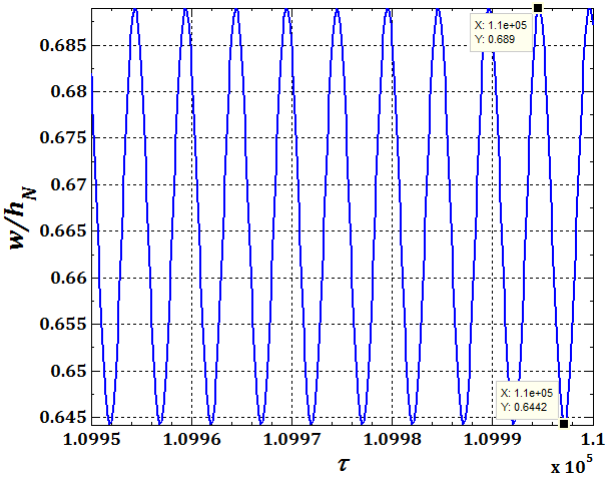

Figure 9. The nonlinear dynamic response of the SS nano resonator under the harmonic excitation

By comparing the static $\left(\bar{w}_s = \frac{(\bar{w}_{max}+\bar{w}_{min})}{2} = 0.6666\right)$ and dynamic $(\bar{w}_d = \frac{(\bar{w}_{max}-\bar{w}_{min})}{2} = 0.0224)$ displacements in the nonlinear dynamic response of Figure 9 and the static and dynamic frequency response of Figure 10 (a, b) at the third resonance frequency $\omega_3 = 1.247$, it can be concluded that the result of this simulation suggests a complete agreement between the numerical and semi-analytical solutions and the averaging method for the FG-PECNS is a suitable method.

In this section, the nonlinear dynamic response convergence of the ode45 method to nano resonator under the harmonic excitation with the material and geometrical parameters Tables 1-3 is investigated. As shown in Figure 11, the nonlinear dynamic response in the radial direction w of the nanoshell in various modes is strongly convergent with increasing the number of modes. The results show that with a constant value of (m) and an increase in the value of (n) there is no change in the motion diagram, for example, $(m = 1, n = 1)$ and $(m = 1, n = 3$ or $n = 5$ and etc) changes are very slight and are overlapping and have the same graph, and only changes in (m) lead to a change in the nonlinear dynamic response graph. In result of, convergence is obtained for the third longitudinal mode $(m = 3)$ and peripheral first mode $(n = 1)$.

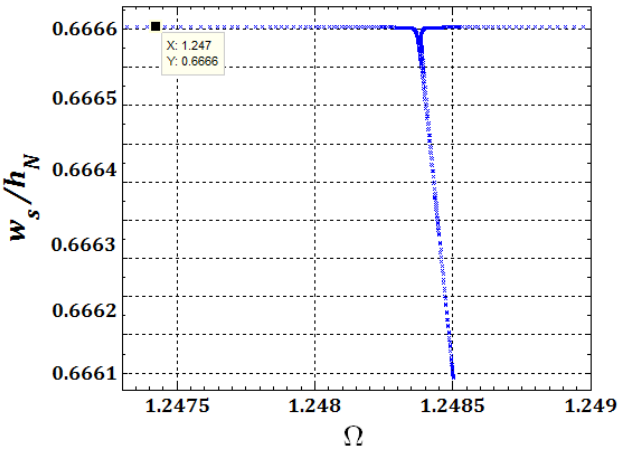

(a) The static frequency response in w direction

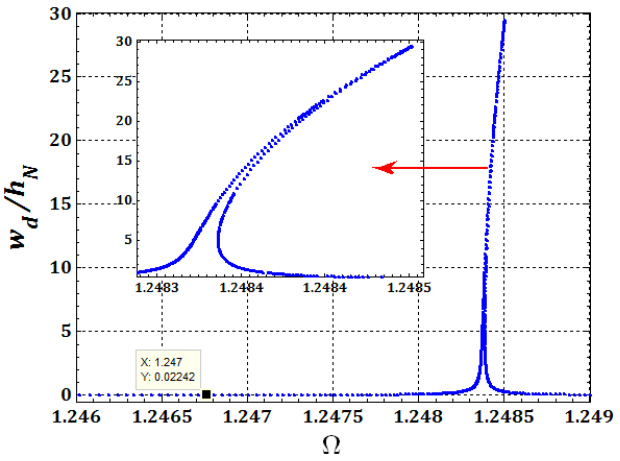

(b) The dynamic frequency response in w direction

Figure 10. The static and dynamic frequency responses of the SS nanoresonator

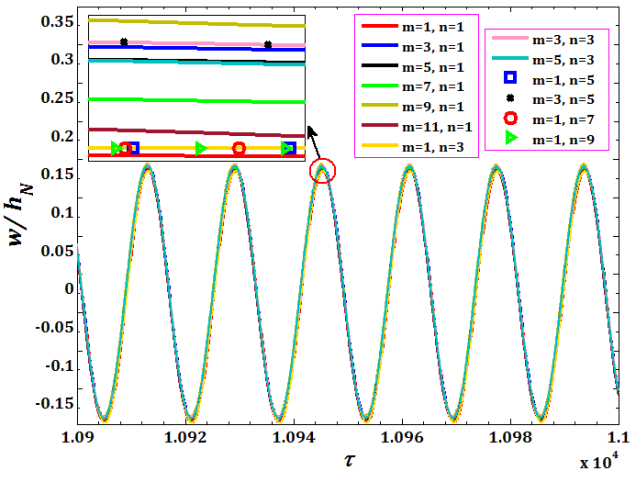

Figure 11. The nonlinear dynamic response convergence of the SS nano-resonator in radial (w) direction

6.3.2. Effects of FG-PCNS parameters on nonlinear frequency response

The main purpose of this section is obtaining analytical solutions of equation for nonlinear frequency response based on arc-length continuation method. For this purpose, the effect of different parameters such as the different boundary conditions, the ratio of the length of the nanosystem to the radius L/R, the ratio of nanoshell thickness to radius h_N/R and the ratio of the piezoelectric thickness to the radius h_p/R, piezoelectric voltage V_p and also amplitude of harmonic excitation will be discussed on the nonlinear frequency response of FG-PCNS.

The nonlinear frequency responses of the piezoelectric nano-shell for different boundary conditions (S-S, C-C, C-S and C-F) are presented in Figure 12. As can be seen, SS and CF boundary conditions respectively have the maximum and minimum resonance amplitude and the frequency responses of the two boundary conditions CC and CS are closely related. Also, the SS boundary condition exhibits stronger nonlinear resonance than the rest, and the CF boundary condition shows a behavior close to linear resonance.

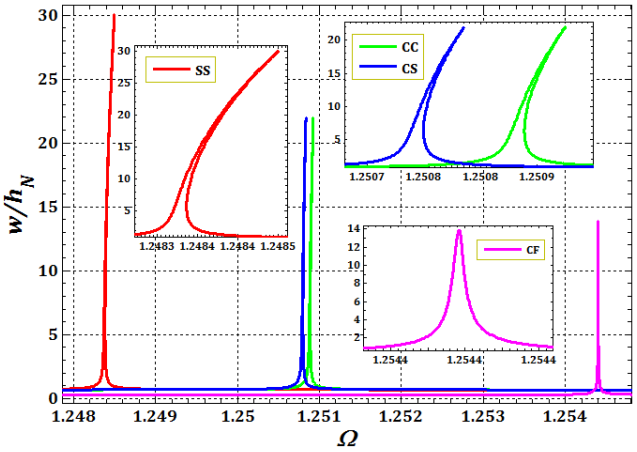

Figure 12. The effect of different boundary conditions on the nonlinear frequency response of the FG-PCNS

In following, for investigation of the nonlinear frequency response, only S-S boundary condition with surface energy effects is considered.

By fixing all parameters except L/R ratio, the results obtained and depicted in Figure 13. This figure shows the effects of L/R ratio on the nonlinear frequency response of the FG-PCNS with five cases $L/R = (5,6,7,8,10)$. As it can be seen, with increasing the length to radius L/R ratio, the resonance will be delayed and resonance amplitude decreases. Also, the lower L/R ratio, the system exhibits more nonlinear behavior i.e. as the ratio of L/R increases, the non-linear resonance effect also decreases. Therefore, it is very important to choose the dimension of the nanoshell.

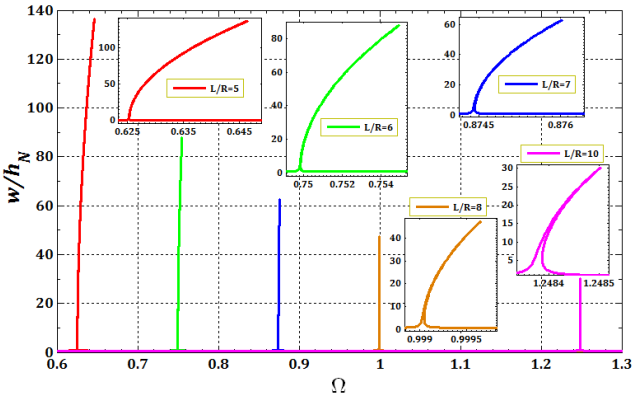

Figure 13. The effects of length to radius L/R ratio on the nonlinear frequency response of the SS FG-PCNS

Figure 14 shows the effects of the ratio shell thickness h_N/R on the nonlinear frequency response of the SS FG-PCNS with different cases of h_N/R. From this figure, we can see that the resonance amplitude of the FG-PCNS decreases when the ratio of h_N/R increase. Also with increasing the h_N/R ratio, the resonance will be delayed and the non-linear resonance behavior also decreases. In other words, the thicker nanoshell has a smaller displacement and the h_N/R has a positive effect on the reduction of the FG-PCNS oscillation amplitude.

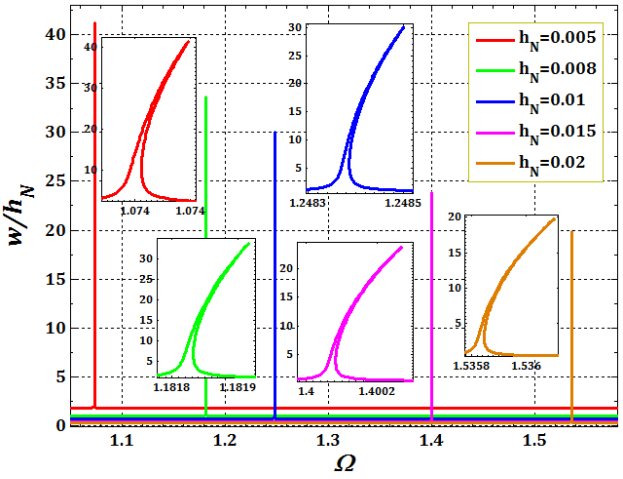

Figure 14. The effect of h_N/R ratio on the nonlinear frequency response of SS FG-PCNS

Figure 15 shows the effects of the ratio piezoelectric thickness h_p/R on the nonlinear frequency response of the SS FG-PCNS with different cases of. Similar to previous Figure, we can see that the amplitude of FG-PCNS frequency

response decreases when the ratio of h_p/R increase, the resonance will be delayed and the non-linear resonance behavior also decreases. In other words, the thicker FG-PCNS have a smaller displacement.

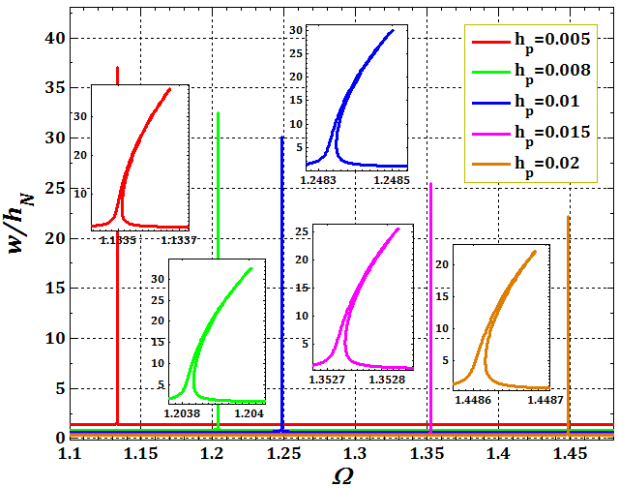

Figure 15. The effect h_p/R ratio on nonlinear frequency response of SS FG-PCNS

Figure 16 presented the effect of piezoelectric voltage V_p on nonlinear frequency response of SS FG-PECNS. It can be seen, as piezoelectric voltage V_p increases, the resonance frequencies and the amplitude of the FG-PECNS increase.

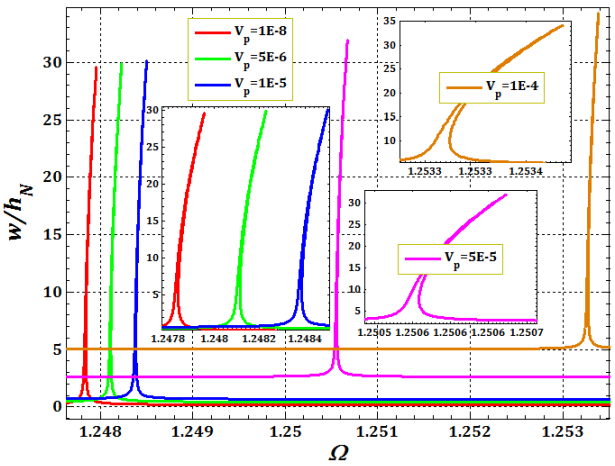

Figure 16. The effect of piezoelectric voltage V_p on nonlinear frequency response of SS FG-PECNS

Finally, the influence of excitation force F on the nonlinear frequency response of the SS FG-PCNS in Figure 17. It can be seen that when F is increased, the value of the FG-PCNS amplitude increases and vice versa and the non-linear resonance behavior also increases.

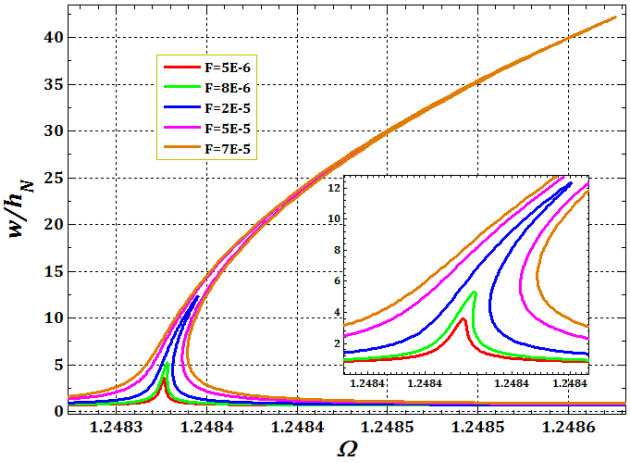

Figure 17. The effect of excitation force F on the nonlinear frequency response of SS FG-PCNS

6. CONCLUSION

In this paper, the oscillatory behavior, nonlinear dynamic and frequency response analysis of functionally graded- piezoelectric cylindrical nano-shell (FG-PCNS) as nanoresonator are investigated with considering of the size-dependent effects. To this end, Gurtin–Murdoch surface elasticity and von karman-Donnell's theory are used. The governing equations and boundary conditions are derived using Hamilton's principle. The assumed mode method is used for changing the partial differential equations into ordinary differential equations. Also, Complex averaging method combined with arc-length continuation is used to achieve an approximate solution for nonlinear frequency response. The validation of the mention system is achieved with excellent agreements by comparisons with numerical results published in the literature. The parametric study such as the effects of geometrical and material properties, different boundary conditions, the ratio of the length of the nanosystem to the radius L/R, the ratio of nanoshell thickness to radius h_N/R, the ratio of the piezoelectric thickness to the radius h_p/R and amplitude of harmonic excitation are conducted on natural frequency, nonlinear dynamic and frequency response of the FG piezoelectric nanoresonator.

Some conclusions are obtained from this study:

- With comparing the previously published in the literature, the present results agree very well with the reference solutions, which indicates that the methods are suitable and of high accuracy for vibration analysis of cylindrical nanoshell.
- For all boundary conditions for as the number of polynomial terms, N, is increased, the value of the frequency parameter, ω_n, converges rapidly and also the convergence mode number is $n = 1$ and $m = 3$.

- In all boundary conditions, the natural frequency decreases with the increase of the L/R ratio.
- With increasing the length to radius ratio L/R, the oscillation amplitude is less but the number of oscillations increases.
- By increasing the thickness shell to small radius ratio h_N/R, the natural frequency increases which in the higher ratio h_N/R, increasing in the frequencies is more evident
- By increasing the ratio h_p/R, the natural frequency increases which in the higher ratio h_p/R, increasing in the frequencies is more evident.
- When F is increased, the value of the FG-PCNS amplitude increases and vice versa.
- The result of this simulation suggests a complete agreement between the numerical and semi-analytical solutions and the averaging method for the FG-PECNS is a suitable method.
- SS and CF boundary conditions respectively have the maximum and minimum resonance amplitude and the frequency responses of the two boundary conditions CC and CS are closely related. Also, the SS boundary condition exhibits stronger nonlinear resonance than the rest, and the CF boundary condition shows a behavior close to linear resonance.
- with increasing the length to radius L/R ratio, the resonance will be delayed and resonance amplitude decreases and in the lower L/R ratio, the system exhibits more nonlinear behavior.
- the resonance amplitude of the FG-PCNS decreases when the ratio of h_N/R increase. Also with increasing the h_N/R and h_p/R ratios, the resonance will be delayed and the non-linear resonance behavior also decreases.
- the amplitude of FG-PCNS frequency response decreases when the ratio of h_p/R increase, the resonance will be delayed and the non-linear resonance behavior also decreases.
- As piezoelectric voltage V_p increases, the resonance frequencies and the amplitude of the FG-PECNS increase.
- when F is increased, the value of the FG-PCNS amplitude increases and vice versa and the non-linear resonance behavior also increases.

REFERENCES

[1] Zhang S.J., Xia R., Lebrun L., Anderson D., Shrout T.R., Piezoelectric materials for high power, high temperature applications, *Materials Letters*, Vol. 59, No.27, 2005, pp. 3471–5.

[2] Manbachi A., Cobbold R.S.C., Development and application of piezoelectric materials for ultrasound generation and detection, *Ultrasound*, Vol.11, No.4, 2011, pp. 187–96.

[3] Jalili N., *Piezoelectric-Based Vibration Control: From Macro to Micro/Nano Scale Systems*, springer, 2010.

[4] Mindlin R.D., Tiersten H.F., Effects of couple-stresses in linear elasticity, *Archive for Rational Mechanics and Analysis*, Vol.11, No.1, 1962, pp. 415–48.

[5] Eringen A.C., Nonlocal polar elastic continua, *International Journal of Engineering Science*, Vol.10, No.1, 1972, pp. 1–16.

[6] Mindlin R.D., Eshel N.N., on first strain-gradient theories in linear elasticity, *International Journal of Solids and Structures*, Vol.4, No.1, 1968, pp. 109–24.

[7] Mindlin R.D., Second gradient of strain and surface-tension in linear elasticity, *International Journal of Solids and Structures*, Vol.1, No.4, 1965, pp. 417–38.

[8] Gurtin M.E., Murdoch A.I., A continuum theory of elastic material surface, *Archive for Rational Mechanics and Analysis*, Vol.57, No.4, 1975, pp. 291–323.

[9] Gurtin M.E., Murdoch A.I., Surface stress in solids, *International Journal of Solids and Structures*, Vol.14, No.6, 1978, pp. 431–40.

[10] Pourkiaee S.M., Khadem S.E., Shahgholi M., Nonlinear vibration and stability analysis of an electrically actuated piezoelectric nanobeam considering surface effects and intermolecular interactions, *Journal of Vibration and Control,* DOI: 10.1177/1077546315603270, 2015.

[11] Pourkiaee S.M., Khadem S.E., Shahgholi M., Parametric resonances of an electrically actuated piezoelectric nanobeam resonator considering surface effects and intermolecular interactions, *Nonlinear Dynamics*, DOI 10.1007/s11071-016-2618-3.

[12] Rouhi H., Ansari R., Darvizeh M., Analytical treatment of the nonlinear free vibration of cylindrical nanoshells based on a first-order shear deformable continuum model including surface influences, *Acta Mechanic*, DOI 10.1007/s00707-016-1595-4.

[13] Fang X.Q., Zhu C.S., Liu J.X., Liu X.L., Surface energy effect on free vibration of nano-sized piezoelectric double-shell structures, *Physica B: Physics of Condensed Matter*, DOI: 10.1016/j.physb.2017.10.038.

[14] Zhu C.S., Fang X.Q., Liu J.X., Surface energy effect on buckling behavior of the functionally graded nano-shell covered with piezoelectric nano-layers under torque, *International Journal of Mechanical Sciences*, Vol.133, 2017, pp. 662–673.

[15] Wang L., Vibration Analysis of Fluid-Conveying Nanotubes with Consideration of Surface Effects, *Physica E: Low-Dimensional Systems and Nanostructures*, Vol.43, 2010, pp. 437–439.

[16] Ghorbanpour Arani A., Fereidoon A., Kolahchi R., Nonlinear surface and nonlocal piezoelasticity theories for vibration of embedded single-layer boron nitride sheet using harmonic differential quadrature and differential cubature methods, *Journal of Intelligent Materials Systems and Structures*, Vol.26, 2015, pp. 1150–1163.

[17] Zhang L.L., Liu J.X., Fang X.Q., Size-dependent dispersion characteristics in piezoelectric nanoplates with surface effects, *Physica E: Low-Dimensional Systems and Nanostructures*, Vol.57, 2014, pp. 169–174.

[18] Fereidoon A., Andalib E., Mirafzal A., Nonlinear Vibration of Viscoelastic Embedded-DWCNTs Integrated with Piezoelectric Layers-Conveying Viscous Fluid Considering Surface Effects, *Physica E: Low-Dimensional Systems and Nanostructures*, Vol.81, 2016, pp. 205–218.

[19] Ghorbanpour Arani A., Kolahchi R., Hashemian M., Nonlocal surface piezoelasticity theory for dynamic stability of double-walled boron nitride nanotube conveying viscose fluid based on different theories, *Proceedings of the Institution of Mechanical Engineers Part C: J Mechanical*

Engineering Science, DOI: 10.1177/0954406214527270, 2014.
[20] Wang K.F., Wang B.L., Effects of residual surface stress and surface elasticity on the nonlinear free vibration of nanoscale plates, *Journal of Applied Physics*, Vol.112, No.1, 2012, pp. 013520–5.
[21] Sahmani S., Aghdam M.M., Bahrami M., Nonlinear buckling and postbuckling behavior of cylindrical shear deformable nanoshells subjected to radial compression including surface free energy effects, *Acta Mechanica Solida Sinica*, Vol.30, No.2, 2017, pp. 209–22.
[22] A Leissa.W., Vibration of Shells, NASA SP 288, US Government Printing Office, 1973, *Reprinted by the Acoustical Society of America*, 1993.
[23] K. Liew M., C Lim.W., Kitipornchai S., Vibration of shallow shells: a review with bibliography, *Applied Mechanics Reviews*, Vol.50, No.8, 1997, pp. 431-444.
[24] Qatu M.S., Sullivan R.W., Wang W., Recent research advances on the dynamic analysis of composite shells: 2000–2009, *Composite Structures*, Vol.93, 2010, pp. 14–31.
[25] Ye T., Jin G., Chen Y., X Ma., Su Z., Free vibration analysis of laminated composite shallow shells with general elastic boundaries, *Composite Structures*, Vol.106, 2013, pp. 470–490.
[26] Fazzolari F.A., A refined dynamic stiffness element for free vibration analysis of cross-ply laminated composite cylindrical and spherical shallow shells, *Composite Structures, Part B*, Vol.62, 2014, pp. 143–158.
[27] S Mirza. and Alizadeh Y., Free vibration of partially supported cylindrical shells, *Shock and Vibration*, Vol.2, No.4, 1995, pp. 297–306.
[28] Loy C. T., Lam K. Y., Shu C., Analysis of cylindrical shells using generalized differential quadrature, *Shock and Vibration*, Vol.4, No.3, 1997, pp.193–198.
[29] Naeem M. N., Sharma C.B., Prediction of natural frequencies for thin circular cylindrical shells, *Proceedings of the Institution of Mechanical Engineers Part C: Journal of Mechanical Engineering Science*, Vol.214, No.10, 2000, pp. 1313–1328.
[30] Donnell L. H., *Beam, Plates and Shells*, McGraw-Hill, New York, 1976.
[31] Amabili M., *Nonlinear Vibrations and Stability of Shells and Plates*, Cambridge University Press, New York, 2008.
[32] Ke, L.L., Wang Y.S., Reddy J.N., Thermo-electro-mechanical vibration of size-dependent piezoelectric cylindrical nanoshells under various boundary conditions, *CompositeStructures*,DOI:http://dx.doi.org/10.1016/j.compstruct.2014.05.048.
[33] Jafari A.A., Khalili S.M.R., Tavakolian M., Nonlinear vibration of functionally graded cylindrical shells embedded with a piezoelectric layer, *Thin- Walled Structures*, Vol.79, 2014, pp. 8–15.
[34] Mohammadimehr M., Rostami R., (2018), Bending and vibration analyses of a rotating sandwich cylindrical shell considering nanocomposite core and piezoelectric layers subjected to thermal and magnetic fields, *Applied Mathematics and Mechanics*, Vol.39, No. 2, 2018, pp.1-22.
[35] A.I. Manevitch, L.I. Manevitch, *Themechanics of Nonlinear Systems with Internal Resonance*, Imperial College Press, London, 2005.
[36] Parseh M., Dardel M., Ghasemi M.H., Pashaei M. H., Steady state dynamics of a non-linear beam coupled to a non-linear energy sink, *International Journal of Non-Linear Mechanics*, Vol. 79, 2016, pp.48–65.

APPENDIX 1

$$\alpha_1 = \frac{1}{m_3}\bar{A}_{11},\ \alpha_2 = \frac{m_0^2}{m_3}\bar{A}_{66},\ \alpha_3 = \frac{m_0}{m_3}(\bar{A}_{12}+\bar{A}_{21}),$$
$$\alpha_4 = \frac{2m_0}{m_3}\bar{A}_{66},\ \alpha_5 = \frac{m_0}{m_3}(\bar{A}_{12}+\bar{A}_{21}),$$
$$\alpha_6 = \frac{1}{2m_1m_3}\left(2\bar{A}_{11}-\bar{\tau}_0^{s_1}-\bar{\tau}_0^{s_2}\right),$$
$$\alpha_7 = \frac{m_0m_2}{2m_3}(\bar{A}_{12}+\bar{A}_{21}),\ \alpha_8 = \frac{2m_0m_2}{m_3}\bar{A}_{66},$$
$$\alpha_9 = \frac{m_0^2}{m_3}\bar{A}_{22}, \alpha_{10} = \frac{m_0^2m_2}{2m_3}\left(2\bar{A}_{22}-\bar{\tau}_0^{s_1}-\bar{\tau}_0^{s_2}\right),$$
$$\alpha_{11} = \frac{m_2}{2m_3}(\bar{A}_{12}+\bar{A}_{21}),\ \alpha_{12} = \frac{m_0^2}{m_3}\left(2\bar{A}_{22}-\bar{\tau}_0^{s_1}-\bar{\tau}_0^{s_2}\right),$$
$$\alpha_{13} = \frac{1}{m_3}\bar{A}_{66},\ \alpha_{14} = \frac{2m_2}{m_3}\bar{A}_{66}, \alpha_{15} = \frac{m_0^2}{m_3}\begin{pmatrix}\bar{A}_{22}-\bar{\tau}_0^{s_1}\\ -\bar{\tau}_0^{s_2}\end{pmatrix},$$
$$\alpha_{16} = \frac{1}{4m_1^2m_3}\begin{pmatrix}\bar{A}_{11}\\ -\bar{\tau}_0^{s_1}-\bar{\tau}_0^{s_2}\end{pmatrix}, \alpha_{17} = \frac{m_0^2m_2^2}{4m_3}\begin{pmatrix}\bar{A}_{22}-\bar{\tau}_0^{s_1}\\ -\bar{\tau}_0^{s_2}\end{pmatrix},$$
$$\alpha_{18} = \frac{m_2^2}{4m_3}\begin{pmatrix}4\bar{A}_{66}\\ +\bar{A}_{12}+\bar{A}_{21}\end{pmatrix}, \alpha_{19} = \frac{m_2}{2m_3}(\bar{A}_{12}+\bar{A}_{21}),$$
$$\alpha_{20} = \frac{m_0^2m_2}{m_3}\left(\bar{A}_{22}-\bar{\tau}_0^{s_1}-\bar{\tau}_0^{s_2}\right),\ \alpha_{21} = -\frac{4m_0m_2}{m_3}\bar{B}_{66},$$
$$\alpha_{22} = \frac{m_0m_2}{m_3}\begin{pmatrix}\bar{F}_{11}-\bar{B}_{12}\\ -\bar{B}_{21}\end{pmatrix}, \alpha_{23} = \frac{1}{m_1m_3}(\bar{F}_{11}-2\bar{B}_{11}),$$
$$\alpha_{24} = \frac{m_2}{m_3}(\bar{F}_{11}-\bar{B}_{12}-\bar{B}_{21}), \alpha_{25} = -\frac{4m_2}{m_3}\bar{B}_{66},$$
$$\alpha_{26} = \frac{m_0^2m_2}{m_3}(\bar{F}_{11}-2\bar{B}_{22}), \alpha_{27} = \frac{m_2^2}{2m_3}\begin{pmatrix}\bar{F}_{11}-\bar{B}_{12}\\ -\bar{B}_{21}\end{pmatrix},$$
$$\alpha_{28} = \frac{m_2}{m_3}(\bar{F}_{11}-\bar{B}_{12}-\bar{B}_{21}), \alpha_{29} = \frac{m_2^2}{2m_3}\begin{pmatrix}\bar{F}_{11}-\bar{B}_{12}\\ -\bar{B}_{21}\end{pmatrix},$$
$$\alpha_{30} = \frac{1}{2m_1^2m_3}\left(\bar{F}_{11}-2\bar{B}_{11}+\bar{\tau}_0^{s_2}(1+m_4)-\bar{\tau}_0^{s_1}\right),$$
$$\alpha_{31} = \frac{m_0^2m_2^2}{2m_3}\left(\bar{F}_{11}-2\bar{B}_{22}+\bar{\tau}_0^{s_2}(1+m_4)-\bar{\tau}_0^{s_1}\right),$$
$$\alpha_{32} = -\frac{4m_2^2}{m_3}\bar{B}_{66},\ \alpha_{33} = \frac{m_0^2m_2}{m_3}\begin{pmatrix}\bar{F}_{11}-2\bar{B}_{22}\\ +\bar{\tau}_0^{s_2}(1+m_4)-\bar{\tau}_0^{s_1}\end{pmatrix},$$
$$\alpha_{34} = \frac{1}{m_1^2m_3}(\bar{D}_{11}-\bar{E}_{11}), \alpha_{35} = \frac{m_0^2m_2^2}{m_3}(\bar{D}_{22}-\bar{E}_{11}),$$
$$\alpha_{36} = \frac{4m_2^2}{m_3}\bar{D}_{66}, \alpha_{37} = \frac{m_2^2}{m_3}(\bar{D}_{12}+\bar{D}_{21}-2\bar{E}_{11}),$$
$$\alpha_{38} = \frac{m_0m_1}{m_3}\left(\bar{\tau}_0^{s_1}+\bar{\tau}_0^{s_2}-\bar{N}_{\theta p}\right), \alpha_{39} = \frac{m_1}{m_3}\begin{pmatrix}\bar{\tau}_0^{s_1}+\bar{\tau}_0^{s_2}\\ -\bar{N}_{xp}\end{pmatrix},$$
$$\alpha_{40} = \frac{m_0m_1}{m_3}\left(\bar{\tau}_0^{s_1}+\bar{\tau}_0^{s_2}-\bar{N}_{\theta p}\right), \alpha_{41} = \frac{1}{2m_3}\begin{pmatrix}\bar{\tau}_0^{s_1}+\bar{\tau}_0^{s_2}\\ -\bar{N}_{xp}\end{pmatrix},$$
$$\alpha_{42} = \frac{m_0^2}{2m_3}\begin{pmatrix}\bar{\tau}_0^{s_1}+\bar{\tau}_0^{s_2}\\ -\bar{N}_{\theta p}\end{pmatrix}, \alpha_{43} = \frac{1}{m_3}\begin{pmatrix}\bar{M}_{xp}+\bar{\tau}_0^{s_1}\\ -\bar{\tau}_0^{s_2}(1+m_4)\end{pmatrix},$$
$$\alpha_{44} = \frac{m_0^2}{m_3}\begin{pmatrix}\bar{M}_{\theta p}+\bar{\tau}_0^{s_1}\\ -\bar{\tau}_0^{s_2}(1+m_4)\end{pmatrix}, \alpha_{45} = -\frac{1}{2m_1^2m_3}\bar{G}_{11}^*,$$
$$\alpha_{46} = -\frac{m_2^2}{2m_3}\bar{G}_{11}^*, \alpha_{47} = \frac{1}{2m_1m_3}\bar{J}_{11}^*, \alpha_{48} = \frac{m_2}{2m_3}\bar{J}_{11}^*,$$
$$\alpha_{49} = \frac{m_2}{2m_3}\bar{J}_{11}^*, \alpha_{50} = \frac{1}{4m_1^2m_3}\bar{J}_{11}^*, \alpha_{51} = \frac{m_2^2}{4m_3}\bar{J}_{11}^*,$$

APPENDIX 2

$$(M)_u^u = \iint\left(\chi_e\chi_i\vartheta_f\vartheta_j\right)d\xi d\theta,$$
$$(M)_u^w = \frac{1}{2}\iint\left(\alpha_{47}\chi_e'\beta_o\vartheta_f\psi_l\right)d\xi d\theta,$$
$$(K)_u^u = \iint\left(\alpha_1\chi_e'\chi_i'\vartheta_f\vartheta_j + \alpha_2\chi_e\chi_i\vartheta_f'\vartheta_j'\right)d\xi d\theta,$$

$$(K)_u^v = \frac{1}{2}\iint \left(\alpha_3 \chi_e' \phi_k \vartheta_f \alpha_l' + \alpha_4 \chi_e \phi_k' \vartheta_f' \alpha_l\right) d\xi d\theta,$$

$$(K)_u^w = \frac{1}{2}\iint \begin{pmatrix} \alpha_5 \chi_e' \beta_o \vartheta_f \psi_l + \alpha_{21} \chi_e \beta_0' \vartheta_f' \psi_l' \\ +\alpha_{22} \chi_e' \beta_o \vartheta_f \psi_l'' + \alpha_{23} \chi_e' \beta_0'' \vartheta_f \psi_l \end{pmatrix} d\xi d\theta,$$

$$(NL)_u^w = \frac{1}{2}\iint \begin{pmatrix} \alpha_6 \chi_e' \beta_0' \beta_t' \vartheta_f \psi_p \psi_v \\ +\alpha_7 \chi_e' \beta_o \beta_t \vartheta_f \psi_p' \psi_v' \\ +\alpha_8 \chi_e \beta_0' \beta_t \vartheta_f' \psi_p \psi_v' \end{pmatrix} d\xi d\theta,$$

$$\bar{F}_{up} = \frac{1}{2}\iint (\alpha_{39} \chi_e' \vartheta_i)\, d\xi d\theta,$$

$$(M)_v^v = \iint \left(\phi_q \phi_k a_f a_l\right) d\xi d\theta,$$

$$(M)_v^w = \frac{1}{2}\iint \left(\alpha_{48} \phi_q \beta_o \alpha_f' \psi_l\right) d\xi d\theta,$$

$$(K)_v^u = \frac{1}{2}\iint \left(\alpha_3 \phi_q \chi_i' \alpha_f' \vartheta_l + \alpha_4 \phi_q' \chi_i \alpha_f \vartheta_l'\right) d\xi d\theta,$$

$$(K)_v^v = \iint \left(\alpha_9 \phi_q \phi_k \alpha_f' \alpha_l' + \alpha_{13} \phi_q' \phi_k' \alpha_f \alpha_l\right) d\xi d\theta,$$

$$(K)_v^w = \frac{1}{2}\iint \begin{pmatrix} \alpha_{12} \phi_q \beta_o \alpha_f' \psi_l + \alpha_{24} \phi_q \beta_0'' \alpha_f' \psi_l \\ +\alpha_{25} \phi_q' \beta_0' \alpha_f \psi_l' + \alpha_{26} \phi_q \beta_o \alpha_f' \psi_l'' \end{pmatrix} d\xi d\theta,$$

$$(NL)_v^w = \frac{1}{2}\iint \begin{pmatrix} \alpha_{10} \phi_q \beta_o \beta_t \alpha_g' \psi_p' \psi_v' \\ +\alpha_{11} \phi_q \beta_0' \beta_t' \alpha_g' \psi_p \psi_v \\ +\alpha_{14} \phi_q' \beta_0' \beta_t \alpha_g \psi_p \psi_v' \end{pmatrix} d\xi d\theta,$$

$$\bar{F}_{vp} = \frac{1}{2}\iint \left(\alpha_{40} \phi_q \alpha_f'\right) d\xi d\theta,$$

$$(M)_w^w = \frac{1}{2}\iint \begin{pmatrix} 2\beta_r \beta_o \psi_s \psi_p + \alpha_{45} \beta_r'' \beta_o \psi_s \psi_p \\ +\alpha_{46} \beta_r \beta_o \psi_s'' \psi_p + \alpha_{49} \beta_r \beta_o \psi_s \psi_p \end{pmatrix} d\xi d\theta,$$

$$(K)_w^u = \frac{1}{2}\iint \begin{pmatrix} \alpha_5 \beta_r \chi_i' \psi_s \vartheta_j + \alpha_{21} \beta_r' \chi_i \psi_p' \vartheta_j' \\ +\alpha_{22} \beta_r \chi_i' \psi_s'' \vartheta_j + \alpha_{23} \beta_r'' \chi_i' \psi_s \vartheta_j \end{pmatrix} d\xi d\theta,$$

$$(K)_w^v = \frac{1}{2}\iint \begin{pmatrix} \alpha_{12} \beta_r \phi_k \psi_s \alpha_l' + \alpha_{24} \beta_r'' \phi_k \psi_s \alpha_l' \\ +\alpha_{25} \beta_r' \phi_k' \psi_s' \alpha_l + \alpha_{26} \beta_r \phi_k \psi_s'' \alpha_l' \end{pmatrix} d\xi d\theta,$$

$$(K)_w^w = \frac{1}{2}\iint \begin{pmatrix} 2\alpha_{15} \beta_r \beta_o \psi_s \psi_p + \alpha_{28} \beta_r \beta_0'' \psi_s \psi_p \\ +\alpha_{28} \beta_r'' \beta_o \psi_s \psi_p + \alpha_{33} \beta_r \beta_o \psi_s \psi_p'' \\ +\alpha_{33} \beta_r \beta_o \psi_s'' \psi_p + 2\alpha_{34} \beta_r'' \beta_0'' \psi_s \psi_p \\ +2\alpha_{35} \beta_o \beta_r \psi_s'' \psi_p'' + 2\alpha_{36} \beta_r' \beta_o' \psi_s' \psi_p' \\ +\alpha_{37} \beta_r \beta_o'' \psi_s'' \psi_p + \alpha_{37} \beta_r'' \beta_o \psi_s \psi_p'' \\ +2\alpha_{41} \beta_r' \beta_o' \psi_s \psi_p + 2\alpha_{42} \beta_r \beta_o \psi_s' \psi_p' \end{pmatrix} d\xi d\theta,$$

$$(K)_{w2}^{\ddot{w}} = \iint \begin{pmatrix} \alpha_{50} \beta_r' \beta_o \beta_t' \psi_s \psi_p \psi_v \\ +\alpha_{51} \beta_r \beta_o \beta_t \psi_s' \psi_p \psi_v' \end{pmatrix} d\xi d\theta,$$

$$(NL)_w^u = \frac{1}{2}\iint \begin{pmatrix} 2\alpha_6 \beta_r' \beta_o' \chi_i' \psi_s \psi_p \vartheta_j \\ +2\alpha_7 \beta_r \beta_o \chi_i' \psi_s' \psi_p' \vartheta_j \\ +\alpha_8 \beta_r' \beta_o \chi_i \psi_s \psi_p' \vartheta_j' \\ +\alpha_8 \beta_r \beta_o' \chi_i \psi_s' \psi_p \vartheta_j' \end{pmatrix} d\xi d\theta,$$

$$(NL)_w^v = \frac{1}{2}\iint \begin{pmatrix} 2\alpha_{10} \beta_r \beta_o \phi_k \psi_s' \psi_p' \alpha_l' + 2\alpha_{11} \beta_r' \beta_o' \phi_k \psi_s \psi_p \alpha_l' \\ +\alpha_{14} \beta_r' \beta_o \phi_k' \psi_s \psi_p' \alpha_l + \alpha_{14} \beta_r \beta_o' \phi_k' \psi_s' \psi_p \alpha_l \end{pmatrix} d\xi d\theta,$$

$$(NL)_{w2}^w = \frac{1}{2}\iint \begin{pmatrix} \alpha_{19} \beta_r \beta_o' \beta_t' \psi_s \psi_p \psi_v + 2\alpha_{19} \beta_r' \beta_o' \beta_t \psi_s \psi_p \psi_v \\ +\alpha_{20} \beta_r \beta_o \beta_t \psi_s \psi_p' \psi_v' + 2\alpha_{20} \beta_r \beta_o \beta_t \psi_s' \psi_p' \psi_v \\ +\alpha_{27} \beta_r'' \beta_o \beta_t \psi_s \psi_p' \psi_v' + 2\alpha_{27} \beta_r \beta_o \beta_t'' \psi_s' \psi_p' \psi_v \\ +\alpha_{29} \beta_r \beta_o' \beta_t' \psi_s'' \psi_p \psi_v + 2\alpha_{29} \beta_r' \beta_o' \beta_t \psi_s \psi_p \psi_v'' \\ +\alpha_{30} \beta_r'' \beta_o' \beta_t' \psi_s \psi_p \psi_v + 2\alpha_{30} \beta_r' \beta_o' \beta_t'' \psi_s \psi_p \psi_v \\ +\alpha_{31} \beta_r \beta_o \beta_t \psi_s'' \psi_p' \psi_v' + 2\alpha_{31} \beta_r \beta_o \beta_t \psi_s' \psi_p' \psi_v'' \\ +\alpha_{32} \beta_r' \beta_o' \beta_t \psi_s' \psi_p \psi_v' + \alpha_{32} \beta_r' \beta_o' \beta_t \psi_s \psi_p' \psi_v' \\ +\alpha_{32} \beta_r \beta_o' \beta_t' \psi_s' \psi_p \psi_v' \end{pmatrix} d\xi d\theta$$

,

$$(NL)_{w3}^w = \iint \begin{pmatrix} 2\alpha_{16} \beta_r' \beta_o' \beta_t' \beta_a' \psi_s \psi_p \psi_v \psi_b \\ +2\alpha_{17} \beta_r \beta_o \beta_t \beta_a \psi_s' \psi_p' \psi_v' \psi_b' \\ +\alpha_{18} \beta_r' \beta_o' \beta_t \beta_a \psi_s \psi_p \psi_v' \psi_b' \\ +\alpha_{18} \beta_r \beta_o \beta_t' \beta_a' \psi_s' \psi_p' \psi_v \psi_b \end{pmatrix} d\xi d\theta,$$

$$\bar{F}_{wp} = \frac{1}{2}\iint (\alpha_{38} \beta_r \psi_s + \alpha_{43} \beta_r'' \psi_s + \alpha_{44} \beta_r \psi_s'')\, d\xi d\theta,$$

$$\bar{F}_H = \iint (\bar{F} \beta_r \beta_s \cos \Omega\tau)\, d\xi d\theta,$$

APPENDIX 3

$$\begin{bmatrix} (\widehat{M})_u^w \\ (\widehat{M})_v^w \end{bmatrix} = \begin{bmatrix} (K)_u^u & (K)_u^v \\ (K)_v^u & (K)_v^v \end{bmatrix}^{-1} \begin{bmatrix} (M)_u^w \\ (M)_v^w \end{bmatrix},$$

$$\begin{bmatrix} (\widehat{K})_u^w \\ (\widehat{K})_v^w \end{bmatrix} = \begin{bmatrix} (K)_u^u & (K)_u^v \\ (K)_v^u & (K)_v^v \end{bmatrix}^{-1} \begin{bmatrix} (K)_u^w \\ (K)_v^w \end{bmatrix},$$

$$\begin{bmatrix} (\widehat{NL})_u^w \\ (\widehat{NL})_v^w \end{bmatrix} = \begin{bmatrix} (K)_u^u & (K)_u^v \\ (K)_v^u & (K)_v^v \end{bmatrix}^{-1} \begin{bmatrix} (NL)_u^w \\ (NL)_v^w \end{bmatrix},$$

$$\begin{bmatrix} \hat{F}_{up} \\ \hat{F}_{vp} \end{bmatrix} = \begin{bmatrix} (K)_u^u & (K)_u^v \\ (K)_v^u & (K)_v^v \end{bmatrix}^{-1} \begin{bmatrix} \bar{F}_{up} \\ \bar{F}_{vp} \end{bmatrix},$$

$$\begin{bmatrix} \hat{F}_{wup} \\ \hat{F}_{wvp} \end{bmatrix} = [(K)_w^u \quad (K)_w^v] \begin{bmatrix} \hat{F}_{up} \\ \hat{F}_{vp} \end{bmatrix},$$

$$\begin{bmatrix} (\widehat{M})_u^{wu} \\ (\widehat{M})_v^{wv} \end{bmatrix} = -[(K)_w^u \quad (K)_w^v] \begin{bmatrix} (\widehat{M})_u^w \\ (\widehat{M})_v^w \end{bmatrix},$$

$$\begin{bmatrix} (\widehat{K})_u^{wu} \\ (\widehat{K})_v^{wv} \end{bmatrix} = -[(K)_w^u \quad (K)_w^v] \begin{bmatrix} (\widehat{K})_u^w \\ (\widehat{K})_v^w \end{bmatrix},$$

$$\begin{bmatrix} (\widehat{NL})_u^{wu} \\ (\widehat{NL})_v^{wv} \end{bmatrix} = -[(K)_w^u \quad (K)_w^v] \begin{bmatrix} (\widehat{NL})_u^w \\ (\widehat{NL})_v^w \end{bmatrix}$$